



**HORIZON 2020**

## **HORIZON 2020 RESEARCH AND INNOVATION FRAMEWORK PROGRAMME OF THE EUROPEAN ATOMIC ENERGY COMMUNITY**

### **Nuclear Fission and Radiation Protection 2018 (NFRP-2018-4)**

Project acronym: **SANDA**

Project full title: **Solving Challenges in Nuclear Data for the Safety of European Nuclear facilities**

Grant Agreement no.: **H2020 Grant Agreement number: 847552**

Workpackage N°: **WP5**

Identification N°: **D5.1**

Type of document: **Deliverable**

Title: **REPORT ON SENSITIVITY ANALYSIS METHODS**

Dissemination Level: **PU**

Reference:

Status: **VERSION 2**

Comments: **Modifications from version 1: correction of the statistical uncertainties calculated with SUMMON and addition of an annex with a list of the sensitivity profiles supplied with this document.**

	Name	Partner	Date	Signature
Prepared by:	V. Bécares	1		
WP leader:	R. Jacqmin	3		
IP Co-ordinator:	E. González	1		

# SANDA Project D5.1: Report on sensitivity analysis methods

V. Bécares<sup>1</sup>, S. Panizo<sup>1</sup>, N. Leclaire<sup>2</sup>, A. Jiménez-Carrascosa<sup>3</sup>, N. García-Herranz<sup>3</sup>, P. Romojaro<sup>1\*</sup>, F. Álvarez-Velarde<sup>1</sup>, O. Cabellos<sup>3</sup>

<sup>1</sup>CIEMAT, Avenida Complutense, 40, 28040 Madrid (Spain).

<sup>2</sup>Institut de Radioprotection et de Sûreté Nucléaire (IRSN), B17, 92262 Fontenay-aux-Roses Cedex (France).

<sup>3</sup>Universidad Politécnica de Madrid (UPM), José Gutiérrez Abascal, 2, 28006 Madrid (Spain).

\* Current address: SCK CEN, Boeretang 200, 2400 Mol (Belgium).

Contact: [vicente.becares@ciemat.es](mailto:vicente.becares@ciemat.es), Tel: +34 91 346 63 85.

## Contents

1. Introduction .....	2
2. Reference system .....	3
3. S/U analysis methodologies.....	5
3.1. Sensitivity coefficients.....	5
3.3.1. TSUNAMI and MCNP sensitivity coefficient calculation methodology .....	6
3.3.2. MORET sensitivity coefficient calculation methodology .....	7
3.2. Uncertainty analysis .....	8
3.2.1. SCALE SAMS and TSAR modules .....	8
3.2.2. SUMMON.....	8
3.2.3. MORET.....	9
4. Intercomparison results.....	10
4.1. Criticality constant.....	10
4.2. Sodium void reactivity worth .....	13
5. Summary and conclusions .....	22
6. Acknowledgements .....	22
7. References .....	22
Annex 1. Sensitivity profiles for $k_{eff}$ .....	24
Annex 2. Sensitivity profiles for $\rho_{void}$ .....	31
Annex 3. Sensitivity data files supplied with this deliverable .....	41

## 1. Introduction

The main purpose of SANDA project Task 5.1 is to analyse the impact of nuclear data uncertainties on design and safety parameters of advanced reactor designs, with the aim of determining the major nuclear data-related sources of uncertainty in reactor parameters, and hence contributing to the improvement of nuclear data libraries. Focus will be on the JEFF-3.3 library, with a view on the next release of this library (JEFF-4.0).

Sensitivity and uncertainty (S/U) analyses play an increasingly important role in modelling and simulation. Sensitivity analysis aims at quantifying the relative dependence of a calculated (output) quantity of interest to the various (input) parameters. Uncertainty analyses or error impact studies, on the other hand, aim at propagating uncertainties or errors in the input model parameters to the calculation results.

In the case of SANDA Task 5.1, the systems being studied are nuclear reactors (from a neutronics point of view), modelled with different neutron transport codes. The output parameters of interest include the criticality constant  $k_{eff}$ , the kinetic parameters ( $\beta_{eff}$  and  $\Lambda_{eff}$ ) and reactivity coefficients. Input parameters include the geometry, material densities and neutron cross sections, which depend on the plant operating conditions (temperature, operating time). Since a complex reactor design contains many materials with a complex isotopic composition, and every isotope can undergo many nuclear reactions, with cross sections extending over a large energy range (usually divided in many energy groups), the number of input parameters of a reactor model, considering only nuclear data, is very large. Furthermore, uncertainty propagation becomes more complex because correlations between the input data (provided in the latest releases of some nuclear data libraries) are usually present and may largely affect the uncertainty propagation results. Therefore, S/U analyses in nuclear reactor systems can be highly complex. As for reactor calculations in general, they have largely benefited from the progress made in computing performance in the last decades.

Different S/U methodologies for nuclear reactor calculations have been developed in recent years, in connection with different neutron transport codes. For this reason, before performing detailed analyses of different systems, it is useful to verify that these different methodologies yield consistent results. In this report, the S/U calculation methodologies of CIEMAT (MCNP + SUMMON), UPM (TSUNAMI) and IRSN (MORET) are described and an intercomparison exercise is conducted.

TSUNAMI is part of the SCALE code package developed and maintained by the Oak Ridge National Laboratory [Rearden 2018]. Processing of nuclear data for use with TSUNAMI-3D is usually performed with the AMPX code, also part of the SCALE package [Wiarda 2016]. SCALE is one of the first neutron transport codes to implement S/U analysis capability and has been widely used as a reference for validating other codes.

MCNP is a Monte Carlo particle transport code developed at Los Alamos National Laboratory [Werner 2017]. MCNP requires the processed nuclear data to be supplied in the ACE format, specifically developed for MCNP. The most widespread code used for this purpose is NJOY [MacFarlane 2016], also developed at Los Alamos National Laboratory. MCNP has several options for performing sensitivity analysis (PERT, KPERT and KSEN cards) but lacks the uncertainty analysis capabilities of TSUNAMI-3D. For this reason, CIEMAT has developed a tool called SUMMON (Sensitivity and Uncertainty Methodology for Monte Carlo codes) [Romojaro 2017] that can use sensitivity profiles calculated with MCNP (and any other code providing that they are in an adequate format) and covariance matrices from the nuclear data libraries to perform uncertainty calculations.

MORET is a Monte Carlo transport code developed at IRSN [Jinaphanh 2016], mainly for criticality safety calculations. It can be used either coupled with the deterministic APOLLO2 code (within the CRISTAL criticality package) as an industrial calculation tool, or alone, in its continuous energy version, as a reference tool like in this work. MORET can use various nuclear data libraries in ACE format; the IRSN GAIA 1.1.2 [Haeck 2015] tool has been developed for producing them. S/U analysis capability based on the Iteration Fission Probability technique (IFP, [Nauchi 2010]) was recently introduced in MORET and allows performing sensitivity calculation for  $k_{eff}$ .

The system chosen for the S/U analysis intercomparison exercise is a simplified RZ model of the ESFR design developed during the ESFR-SMART project of H2020 (section 2). This model was chosen for its simplicity and easy implementation within the three codes. The model is available through the OECD-NEA and has been

subjected to previous S/U analysis, therefore it is well known. The parameters for which S/U analysis have been performed are the criticality constant  $k_{eff}$  (section 4.1) and the sodium void reactivity coefficient  $\rho_{void}$  (section 4.2). All calculations have been performed with the JEFF-3.3 library.

We stress that the aim of this exercise is not to focus on the results for this particular simplified ESFR model (this is the objective of other deliverables within this task), but rather on the S/U methodology itself, to guarantee the consistency of the results obtained with different methodologies.

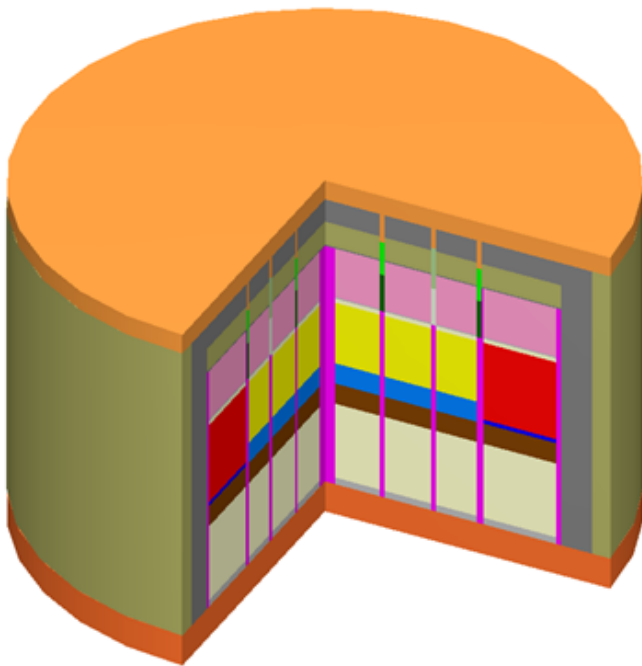
## 2. Reference system

The system chosen for the intercomparison exercise is a simplified, RZ model of the ESFR at End-of-Cycle (EoC) developed by UPM within Task 1.2.2 of the H2020 ESFR-SMART program [Mikityuk 2017] for the specific purpose of S/U analysis. The model is also being used by OECD-NEA WPEC/SG46 [Jiménez-Carrascosa 2020].

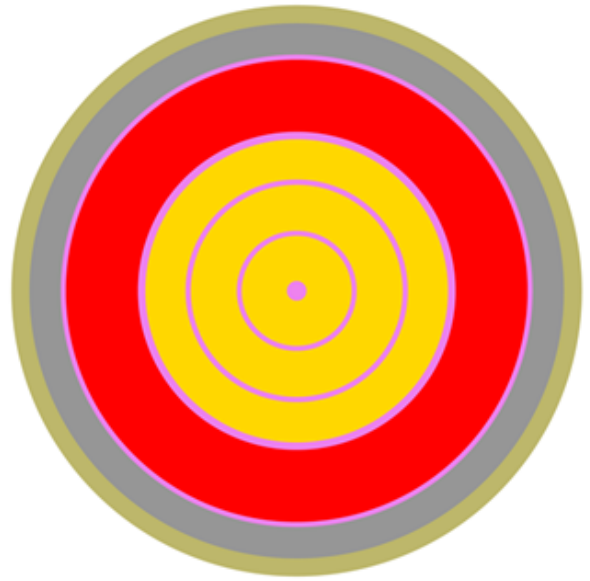
The choice of an RZ model has been made over a detailed 3D model based on previous experience during the ESFR-SMART project. Within this project, it was found that the computational requirements (memory, computational time) to perform S/U calculations with a detailed 3D model of the same core were very high, leading to results affected by large statistical errors or even the impossibility to get converged calculations. Furthermore, this simplified geometry is easier to implement in neutron transport codes. Since we focus here on the intercomparison of results obtained with different methodologies, and not on the results themselves, the differences between the 3D model and the RZ model have not been analysed.

The model (Figure 1) consists of a MOX core that is divided in inner and outer core regions. These inner and outer cores are further divided into a fissile region at the top and a fertile region at the bottom. The fuel region is made two radial zones having different plutonium fractions, and is radially surrounded by a sodium reflector. There is a sodium plenum above the fuel.  $B_4C$  control rods are modelled as cylindrical regions. The dimensions (radii) of the homogenized regions have been calculated to preserve the material masses with respect to the full 3D configuration. For simplicity, only two material temperatures are considered (900 and 1200 K).

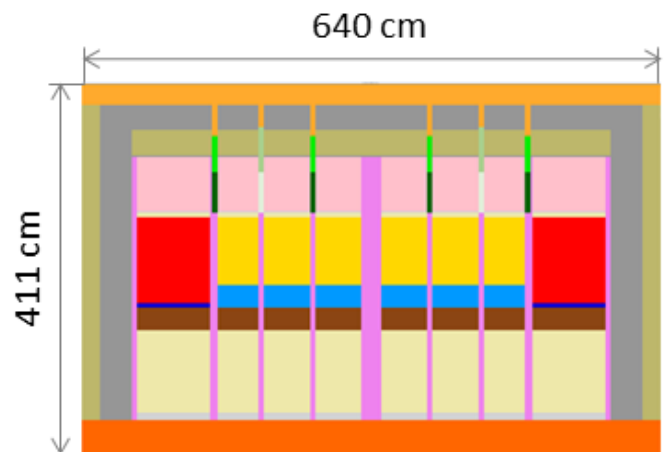
The model represents the End-of-Cycle (EoC) conditions. This corresponds to the most limiting situation concerning sodium voiding [Davies 2020]. The complex material composition poses some computational challenges, in spite of the simplified geometry, but on the other hand it allows for a higher number of isotopes and reactions to be compared between the institutions participating in the exercise.



(a) 3D view



(b) Horizontal section



(c) Vertical section

- Inner core. Fissile fuel
- Outer core. Fissile fuel
- Inner core. Fertile fuel
- Outer core. Fertile fuel
- Reflector
- Plug
- Sodium plenum
- Absorber
- Gas plenum
- Header
- Footer

- Steel blanket
- Follower: sodium plenum
- CSD enriched absorber
- CSD natural absorber
- DSD enriched absorber
- DSD natural absorber

Figure 1. ESFR RZ model.

### 3. S/U analysis methodologies

#### 3.1. Sensitivity coefficients

The *sensitivity coefficient* of a model output parameter  $k$  to an input parameter  $\alpha$  is defined as:

$$S_{\alpha} = \frac{\alpha}{k} \left( \frac{\partial k}{\partial \alpha} \right) \quad (3.1)$$

In reactor physics, the output parameter  $k$  is a reactor integral quantity of interest (e.g. the criticality constant  $k_{eff}$ , the kinetic parameters  $\beta_{eff}$  or  $\Lambda_{eff}$  or a reactivity coefficient) while the input parameter  $\alpha$  is a neutron cross section or, more specifically, the value of the cross section in a certain energy range. A set of sensitivity coefficients  $S_{k,\alpha}$  calculated over a range of energy groups is referred as a *sensitivity profile*.

There are three major approaches for the calculation of sensitivity coefficients [Kiedrowski 2011a, Rearden 2011]:

1. The *direct perturbation technique* simply performs two independent calculations for  $k$ , with the original (unperturbed) set cross sections  $\alpha^0$  and a perturbed one  $\alpha$ . Assuming that the perturbation is small enough so that system response can be considered linear we have that:

$$S_{\alpha} = \frac{\alpha^0}{k(\alpha^0)} \left( \frac{k(\alpha) - k(\alpha^0)}{\alpha - \alpha^0} \right) \quad (3.2)$$

The major difficulty in applying this technique with Monte Carlo codes is that it requires the calculation of the difference between two very similar numbers ( $k(\alpha)$  and  $k(\alpha_0)$ ), for which highly precise results are needed, which in turn requires large computational resources. Furthermore, it requires an independent calculation for every single input parameter. This often makes this technique impractical and has prompted the development of alternative techniques. However, the direct perturbation technique is still useful to validate these alternative techniques.

2. The *differential operator technique* is based on a Taylor series expansion of  $k$ . The variation  $\Delta k$  for a given  $\Delta \alpha$  is obtained from the evaluation of partial derivatives, usually truncated to first or second order:

$$\Delta k = \sum_i \left( \frac{\partial k}{\partial \alpha_i} \right)_{\alpha^0} \Delta \alpha_i + \frac{1}{2} \sum_{i,j} \left( \frac{\partial^2 k}{\partial \alpha_i \partial \alpha_j} \right)_{\alpha^0} \Delta \alpha_i \Delta \alpha_j + \dots \quad (3.3)$$

The challenge in applying this method with Monte Carlo codes is evaluating the derivatives, which have to be tallied for every neutron history. This methodology is available in the PERT card of MCNP and has been found to be accurate for fixed source problems but much less so for eigenvalue problems. This is because it does not take into account the perturbation in the fission source, only the perturbation in the cross sections. MORET also applies a combination of the differential operator technique with the adjoint-flux weighted perturbation technique for calculating sensitivity coefficients of  $k_{eff}$ .

3. The *adjoint-flux-weighted perturbation technique* makes use of perturbation theory. In first order perturbation theory (i.e. assuming linearity), the variation in the reactivity of the system  $\Delta \rho$  as a consequence of a perturbation  $\Delta \hat{F}$  in the fission (creation) operator  $\hat{F}$  or a perturbation  $\Delta \hat{M}$  in the migration and losses (destruction) operator  $\hat{M}$  is given by:

$$\Delta \rho = - \frac{\langle \phi_0^+, [\Delta \hat{M} - \frac{1}{k} \Delta \hat{F}] \phi_0 \rangle}{\langle \phi_0^+, \hat{F}_0 \phi_0 \rangle} \quad (3.4)$$

Where  $\phi_0$  and  $\phi_0^\dagger$  denote, respectively, the neutron flux and the adjoint neutron flux in the initial (unperturbed) state. The main difficulty in applying this technique with Monte Carlo codes is the calculation of the adjoint flux, especially with continuous-energy codes. For this purpose, several methodologies have been developed in recent years. The adjoint-flux-weighted perturbation technique is available in TSUNAMI-3D, MCNP KPERT and KSEN cards and, as stated above, in MORET.

From the sensitivity coefficient of the criticality constant, it is straightforward to derive the sensitivity coefficient of the reactivity responses. If the sensitivity coefficients  $S_{\alpha,1}$  and  $S_{\alpha,2}$  in two configurations are known, we have that:

$$S_{\rho_{1 \rightarrow 2}, \alpha} = \frac{\alpha}{\rho_{1 \rightarrow 2}} \frac{\partial \rho_{1 \rightarrow 2}}{\partial \alpha} = \frac{\alpha}{\rho_{1 \rightarrow 2}} \left( \frac{\partial \lambda_1}{\partial \alpha} - \frac{\partial \lambda_2}{\partial \alpha} \right) = \frac{\lambda_1 S_{\alpha,1} - \lambda_2 S_{\alpha,2}}{\rho_{1 \rightarrow 2}} \quad (3.5)$$

where  $\rho_{1 \rightarrow 2}$  denotes the reactivity response (assumed to be non-zero) and  $\lambda = 1/k$ . The sensitivity of the kinetic parameters to the cross sections can be obtained in a similar way, see for instance [Romojaro 2019].

### 3.3.1. TSUNAMI and MCNP sensitivity coefficient calculation methodology

As stated above, the SCALE code package is one of the first widespread nuclear calculation systems that offered a S/U calculation capability. This was achieved through the TSUNAMI (*Tools for Sensitivity and Uncertainty Analysis Methodology Implementation*) module. Actually, different versions of this module are available: TSUNAMI-1D, coupled to the one-dimensional deterministic XSDRNPM particle transport code; TSUNAMI-2D, coupled to the two-dimensional deterministic NEWT transport core; and TSUNAMI-3D, coupled to the three-dimensional Monte Carlo KENO particle transport code in both multigroup (MG) and continuous energy (CE) approaches. All mentioned transport codes are part of the SCALE package themselves. It was also SCALE that introduced the *Sensitivity Data File* (.sdf) format that has become a standard format for sensitivity data exchange. For details about this format, see [Rearden 2018] pp. 6-318 to 6-319.

TSUNAMI-1D, TSUNAMI-2D and MG TSUNAMI-3D methodology for sensitivity calculation are based on the adjoint-weighted perturbation theory. This methodology applies Eq. 3.4 in a multi-group approach [Rearden 2011]. The energy, the space and the angular momenta are discretized and the forward and adjoint fluxes are tallied for every space, energy and angular momentum region. An issue with this multi-group approach is calculating the sensitivities of resonance self-shielded cross sections; the BONAMIST module (based on the BONAMI module) is used for that purpose.

In addition to this multi-group methodology, TSUNAMI-3D offers the option of performing continuous-energy S/U calculations. Two methodologies are available for evaluating the adjoint flux: the *Iterated Fission Probability* (IFP) methodology and the *Contribution-Linked eigenvalue sensitivity/Uncertainty estimation via Track-length importance Characterization* (CLUTCH) methodology. MCNP applies the same methodology as continuous-energy TSUNAMI-3D, but only the IFP methodology is available for calculating the adjoint flux. MCNP has two cards that implement this methodology, namely KPERT and KSEN. The difference between them is the treatment of scattering laws; the KPERT methodology has been found to be inadequate for calculating scattering sensitivities [Kiedrowski 2010, Kiedrowski 2012]. All sensitivity coefficients presented here have been calculated with the KSEN card. As commented before, MCNP also has the PERT card that applies the differential operator technique, but this card is only recommended for fixed source problems, since it does not take into account the perturbations in the fission source.

The IFP methodology [Kiedrowski 2011b] is based on the interpretation of the adjoint flux as neutron importance, i.e., as the number of fissions (or progeny) that are originated by a given neutron within the system. With this methodology, the adjoint flux at a given point of the phase space  $x_N$  is evaluated as the number of neutrons originated from an initial neutron at  $x_N$  after a given number of generations. This number of generations is called *latent generations* in TSUNAMI and *block* in MCNP. It can be defined by the user both in

TSUNAMI and MCNP (BLOCKSIZE option of the KOPTS card). In this work, the default value of 10 generations has been used.

The calculations required by the IFP technique are performed alongside the criticality calculation. In this way, no extra computing time is required, but the extra memory requirements may become an issue, however. In order to reduce these memory requirements, the CLUTCH methodology [Perfetti 2016] has been developed. The CLUTCH methodology has also been implemented in the MORET code [Jinaphanh 2017], but it is not available in the production version. Nevertheless, the IFP methodology makes fewer assumptions and is retained in TSUNAMI as a reference for validating the CLUTCH methodology.

For calculating the sensitivity coefficients of the reactivity responses, TSUNAMI uses a SCALE module named *Tool for Sensitivity Analysis of Reactivity Responses* (TSAR). MCNP does not have any tool for computing these sensitivity coefficients. This is one of the capabilities of the SUMMON code.

### 3.3.2. MORET sensitivity coefficient calculation methodology

The methodology used by MORET to calculate sensitivity coefficients, first implemented in the 5.C.1 release [Jinaphanh 2016] is a combination of the differential operator technique, applied to determine the impact on the perturbation in the cross sections, with an IFP based methodology to calculate the impact of the perturbation in the fission source. With this methodology, MORET can calculate sensitivity coefficients of  $k_{eff}$  to the total (MT = 1), elastic scattering (MT = 2), total inelastic scattering (MT = 4), total scattering (MT = 1003, in MORET denomination), total fission (MT = 18), total capture (MT = 101) and radiative capture (MT = 102) cross sections, in addition to the average number of neutrons produced by fission (MT = 452), the fission spectrum (MT = -1018) and the elastic scattering (MT = -1002) and total inelastic scattering laws (MT = -1004). For the moment, however, MORET does not have the capability to calculate sensitivity coefficients to other quantities than  $k_{eff}$ .

The differential operator technique in MORET is truncated to the first order in the derivatives. These derivatives are derived from computed cycle (batch) estimators. Let us denote  $k_0$  the contribution to  $k_{eff}$  at a given cycle:

$$k_0 = \sum_j p_j \times \xi_j \quad (3.6)$$

$\xi_j$  is an estimator of  $k_{eff}$ , e.g. the absorption estimator:

$$\xi_j = \frac{v\sigma_f(x_N)}{\sigma_a(x_N)} \quad (3.7)$$

with  $x_N$  the phase-space coordinates of the last collision.  $p_j$  is the probability of occurrence of history  $j$ , which is in turn given by:

$$p_j = Q_0(r_0) \frac{F(r_0, E'_0 \rightarrow E_0)}{4\pi} T(r_0 \rightarrow r_1) \prod_{n=1}^{N-1} K(x_n \rightarrow x_{n+1}) a(x_N) \quad (3.8)$$

where  $Q_0$  is the fission source operator,  $F$  is the fission spectrum operator,  $K = CT$  is the transport operator with  $C$  and  $T$  the collision and translation operators, respectively, and  $a$  is the absorption operator. The index  $n$  ranges over the collisions and  $x_n$  are the phase-space coordinates of the collisions.

The first derivative of (3.6) with respect to a cross section  $\alpha$  is given by:

$$k'_0 = \frac{\partial k_0}{\partial \alpha} = \sum_j p'_j \times \xi_j + p_j \times \xi'_j = \sum_j p_j \times \mu_j \quad (3.9)$$

Where  $\mu_j$  denotes the following expression:

$$\mu_j = \left[ \frac{Q'_0(r_0)}{Q_0(r_0)} + \frac{F'(r_0, E'_0 \rightarrow E_0)}{F(r_0, E'_0 \rightarrow E_0)} + \frac{T'(r_0 \rightarrow r_1)}{T(r_0 \rightarrow r_1)} + \sum_n \frac{C'(E_n, \Omega_n \rightarrow E_{n+1}, \Omega_{n+1})}{C(E_n, \Omega_n \rightarrow E_{n+1}, \Omega_{n+1})} + \sum_n \frac{T'(r_n \rightarrow r_{n+1})}{T(r_n \rightarrow r_{n+1})} + \frac{a'}{a} + \frac{\xi'_j}{\xi_j} \right] \xi_j \quad (3.10)$$

It is possible to obtain analytic expressions for all the terms in the RHS of Eq. 3.10 except for the fission source term,  $Q'_0(r_0)/Q_0(r_0)$ . For this term, there is a methodology proposed in [Blyskavka 2005], which is based on replacing the first derivatives by an estimation of the adjoint fission source:

$$S_{\alpha}^{f.s.} = \frac{\alpha}{k_0} \sum_j p_j \frac{Q_{r_0}(r_0)}{Q_0(r_0)} \xi_j = \frac{\sum_j p_j \alpha \mu_0 \xi_j Q^{\dagger}(r_N)}{\sum_j p_j \xi_j Q^{\dagger}(r_N)} \quad (3.11)$$

where  $Q^{\dagger}(r_N)$  denotes the adjoint source at the location  $r_N$ . This adjoint source is related to the fission source spectrum  $\chi$  and the adjoint flux  $\phi^{\dagger}(x)$  by the expression:

$$Q^{\dagger}(r_N) = \left\langle \frac{1}{4\pi} \chi(x) \phi^{\dagger}(x) \right\rangle_{E,\Omega} \quad (3.12)$$

The adjoint flux is in turn calculated with the IFP methodology described in Section 3.3.1.

### 3.2. Uncertainty analysis

As stated above, the aim of uncertainty analyses is to propagate the uncertainty in the input model parameters (in this case the nuclear data) to the calculation results. Latest versions of nuclear data libraries, including JEFF, include information about the uncertainty in the reaction cross sections, in the form of covariance matrices. These matrices contain the covariance between the cross section values in a pair of energy groups. Covariances between different reactions for a given isotope are also supplied; covariance between reactions for different isotopes has yet to be provided in any library as far as we know.

With the knowledge of the sensitivity profiles  $S_{\alpha}$  and the covariance matrix  $V_{\alpha}$ , the contribution to the variance of a given reaction can be obtained as:

$$\sigma^2 = S_{\alpha} V_{\alpha} S_{\alpha}^T \quad (3.13)$$

Because of its shape, Eq. 3.12 is known as the *sandwich rule* (e.g. [Cacuci 2003]).

#### 3.2.1. SCALE SAMS and TSAR modules

Within the SCALE code system, uncertainty analysis is performed with the Sensitivity Analysis Module for SCALE (SAMS) applying the sandwich rule. Furthermore, the TSAR module also performs uncertainty calculations for reactivity differences.

#### 3.2.2. SUMMON

The SUMMON code [Romero 2017] has been developed at CIEMAT with the aim to couple .sdf files and covariance matrices from different sources to perform uncertainty calculations (Figure 2)<sup>1</sup>. SUMMON can also perform eigenvalue-difference response calculations. In this way, it offers the functionalities of the SAMS and TSAR modules of SCALE. Furthermore, SUMMON can also perform S/U analysis for the kinetic parameters,  $\Lambda_{eff}$  and  $\beta_{eff}$ . In this work, SUMMON has been applied with sensibility profiles calculated with the KSEN card of MCNP and the covariance matrices from JEFF-3.3. Furthermore, it has also been applied with sensitivity profiles calculated with TSUNAMI-3D (in addition to SAMS and TSAR modules) and MORET.

---

<sup>1</sup> SUMMON 2.4c has been used in version 2 of this report. Compared with the previous version of SUMMON used in version 1 of this report, SUMMON 2.4c has an improved algorithm for propagating the statistical uncertainties in the sensitivity profiles  $S_{\alpha}$  to the result of the sandwich rule  $\sigma$ .

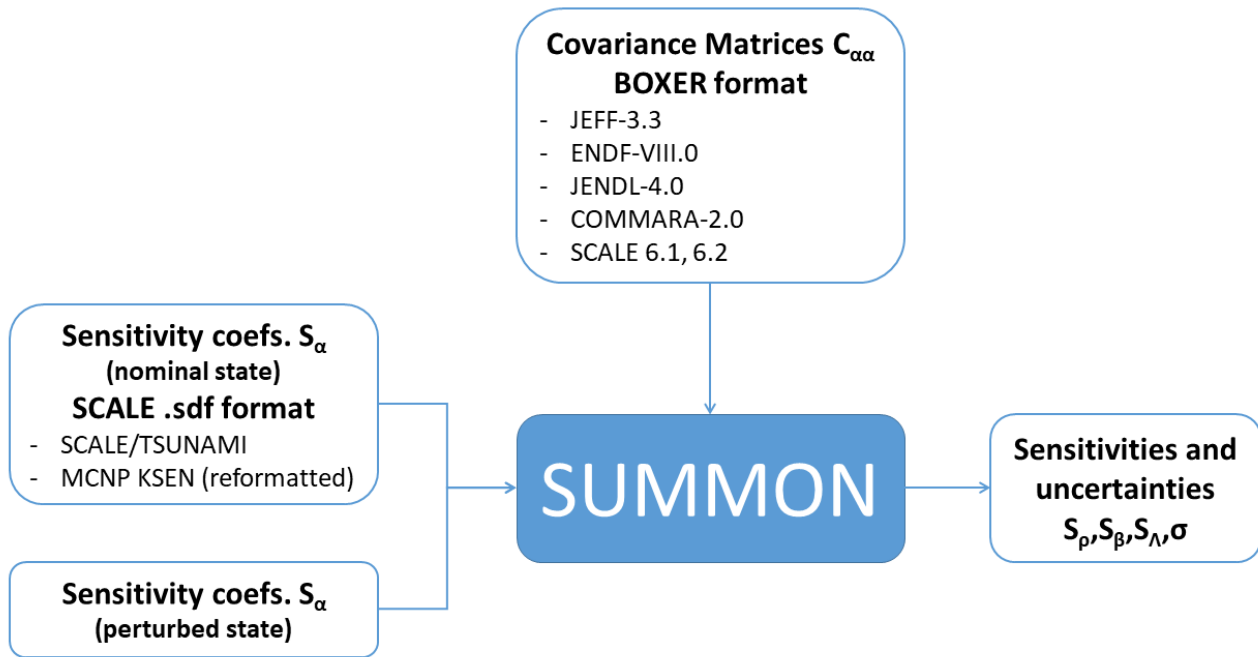


Figure 2. Schematics of SUMMON operation.

### 3.2.3. MORET

MORET does not have the capability to carry out uncertainty calculations by itself. Therefore, uncertainty calculations have to be performed with external tools such as MACSENS (*Moret helper tool for Characterization and SENSitivity Studies*) of IRSN. This tool uses the sandwich rule to perform prior uncertainty calculations (due to nuclear data covariance matrix), as it is the case with the SUMMON and SAMS packages. Furthermore, MACSENS can make posterior uncertainty calculations (using GLLSM methodology and sensitivity coefficients calculated by MORET and covariance data). In this work, however, as stated above, SUMMON has been used (instead of MACSENS) with MORET sensitivity profiles to obtain uncertainty values.

## 4. Intercomparison results

### 4.1. Criticality constant

The results of the S/U analysis for the  $k_{eff}$  of the ESRF configuration described in Section 2, performed with the MCNP, TSUNAMI-3D and MORET codes, are presented in this section.

As stated above, the JEFF-3.3 library has been used with all three codes. In the case of MCNP, it has been processed with the NJOY2012.84 code at the temperatures of the model (900 and 1200 K). The covariance matrices in 33-group structure have been processed with the NJOY21 code. The processing is based on NEA's NJOY inputs. In the case of CE TSUNAMI-3D, the JEFF-3.3 library has been processed with the AMPX code using the latest updates in SCALE6.3beta version. For MORET, the JEFF-3.3 library has been processed at 900 and 1200 K using the IRSN GAIA 1.1.2 tool mentioned in Section 1. This tool is a wrapper of NJOY2016.35 that produces ACE formatted nuclear data (cross sections and thermal scattering data) through a given sequence of NJOY modules and makes additional tests on the NJOY results (e.g. consistency between total cross sections and sum of partial cross sections).

The values of  $k_{eff}$  obtained with the three codes are:

$$k_{eff,MCNP} = 1.00036 \pm 0.00008$$

$$k_{eff,KENO} = 1.00016 \pm 0.00008$$

$$k_{eff,MORET} = 1.00041 \pm 0.00020$$

Table 1. Reactions with the largest Integrated Sensitivity Coefficients for the keff of ESRF.

ESFR-RZ -33 energy groups					
Sensitivity (keff) - Integrated sensitivity values					
Reaction	TSUNAMI-3D	MCNP		MORET	
		Result	Ratio	Result	Ratio
$^{239}\text{Pu}$ (n,f)	4.776E-01 $\pm$ 7.331E-05	4.777E-01 $\pm$ 1.452E-03	1.000 $\pm$ 0.003	4.628E-01 $\pm$ 1.414E-03	0.969 $\pm$ 0.003
$^{238}\text{U}$ (n, $\gamma$ )	-1.932E-01 $\pm$ 3.297E-05	-1.912E-01 $\pm$ 3.293E-04	0.990 $\pm$ 0.002	-1.776E-01 $\pm$ 1.795E-04	0.919 $\pm$ 0.001
$^{241}\text{Pu}$ (n,f)	7.759E-02 $\pm$ 4.224E-05	7.789E-02 $\pm$ 2.681E-04	1.004 $\pm$ 0.003	7.648E-02 $\pm$ 5.840E-04	0.986 $\pm$ 0.008
$^{238}\text{U}$ (n,f)	7.513E-02 $\pm$ 4.972E-05	7.518E-02 $\pm$ 5.206E-04	1.001 $\pm$ 0.007	7.123E-02 $\pm$ 6.180E-04	0.948 $\pm$ 0.008
$^{238}\text{U}$ (n,n')	-7.151E-02 $\pm$ 1.252E-04	-6.957E-02 $\pm$ 1.909E-03	0.973 $\pm$ 0.027	-6.775E-02 $\pm$ 1.542E-03	0.947 $\pm$ 0.022
$^{16}\text{O}$ (n,n)	-6.270E-02 $\pm$ 7.738E-04	-5.746E-02 $\pm$ 5.513E-03	0.916 $\pm$ 0.089	-6.861E-02 $\pm$ 4.489E-03	1.094 $\pm$ 0.080
$^{240}\text{Pu}$ (n,f)	5.591E-02 $\pm$ 4.022E-05	5.624E-02 $\pm$ 2.359E-04	1.006 $\pm$ 0.004	5.594E-02 $\pm$ 4.995E-04	1.001 $\pm$ 0.009
$^{239}\text{Pu}$ (n, $\gamma$ )	-4.018E-02 $\pm$ 1.070E-05	-3.958E-02 $\pm$ 1.060E-04	0.985 $\pm$ 0.003	-3.824E-02 $\pm$ 5.918E-05	0.952 $\pm$ 0.001
$^{240}\text{Pu}$ (n, $\gamma$ )	-2.487E-02 $\pm$ 5.360E-06	-2.486E-02 $\pm$ 6.045E-05	1.000 $\pm$ 0.002	-2.482E-02 $\pm$ 3.810E-05	0.998 $\pm$ 0.002
$^{56}\text{Fe}$ (n,n')	-2.136E-02 $\pm$ 5.696E-05	-2.120E-02 $\pm$ 8.179E-04	0.992 $\pm$ 0.038	-2.016E-02 $\pm$ 6.475E-04	0.944 $\pm$ 0.030
$^{238}\text{U}$ (n,n)	1.114E-05 $\pm$ 2.079E-05	1.427E-02 $\pm$ 5.412E-03	1281 $\pm$ 2439	1.216E-02 $\pm$ 4.463E-03	1091 $\pm$ 2075
$^{56}\text{Fe}$ (n, $\gamma$ )	-1.015E-02 $\pm$ 5.737E-06	-9.466E-03 $\pm$ 8.767E-05	0.933 $\pm$ 0.009	-7.324E-03 $\pm$ 5.829E-05	0.722 $\pm$ 0.006
$^{241}\text{Pu}$ (n, $\gamma$ )	-4.341E-03 $\pm$ 9.355E-07	-4.353E-03 $\pm$ 9.775E-06	1.003 $\pm$ 0.002	-4.344E-03 $\pm$ 5.446E-06	1.001 $\pm$ 0.001
$^{240}\text{Pu}$ (n,n')	-2.646E-03 $\pm$ 2.225E-05	-2.566E-03 $\pm$ 3.982E-04	0.970 $\pm$ 0.151	-2.681E-03 $\pm$ 3.423E-04	1.013 $\pm$ 0.130

$^{238}\text{Pu}$ (n, $\gamma$ )	-2.485E-03 $\pm 6.633\text{E-}07$	-2.496E-03 $\pm 7.946\text{E-}06$	1.005 $\pm 0.003$	-2.494E-03 $\pm 5.584\text{E-}06$	1.004 $\pm 0.002$
$^{239}\text{Pu}$ (n,n')	-3.288E-03 $\pm 2.640\text{E-}05$	-2.424E-03 $\pm 4.799\text{E-}04$	0.737 $\pm 0.146$	-2.825E-03 $\pm 4.154\text{E-}04$	0.859 $\pm 0.127$
$^{56}\text{Fe}$ (n,n)	-2.139E-04 $\pm 9.937\text{E-}04$	1.601E-03 $\pm 4.626\text{E-}03$	-7.5 $\pm 41$	-1.060E-02 $\pm 3.475\text{E-}03$	50 $\pm 231$
$^{23}\text{Na}$ (n, $\gamma$ )	-1.513E-03 $\pm 6.426\text{E-}07$	-1.426E-03 $\pm 7.471\text{E-}06$	0.943 $\pm 0.005$	-8.508E-04 $\pm 3.005\text{E-}06$	0.562 $\pm 0.002$
$^{240}\text{Pu}$ (n,n)	4.934E-04 $\pm 8.649\text{E-}05$	1.147E-03 $\pm 1.460\text{E-}03$	2.3 $\pm 3.0$	-5.575E-04 $\pm 1.172\text{E-}03$	-1.13 $\pm 2.38$
$^{104}\text{Ru}$ (n, $\gamma$ )	-5.875E-04 $\pm 1.983\text{E-}07$	-5.855E-04 $\pm 3.372\text{E-}06$	0.997 $\pm 0.006$	-5.729E-04 $\pm 2.357\text{E-}06$	0.975 $\pm 0.004$
$^{238}\text{U}$ (n,2n)	1.702E-03 $\pm 5.597\text{E-}06$	4.234E-04 $\pm 1.052\text{E-}04$	0.249 $\pm 0.062$	---	---

lists the reactions with the largest Integrated Sensitivity Coefficients (ISCs) obtained with all three codes. In Annex 1, figures of the sensibility profiles of all these reactions are presented. Ratios with the TSUNAMI-3D results are also listed for MCNP and MORET. It can be observed that in most cases the difference between the codes are small, up to a few percent, and compatible within statistical errors in many cases. There are however some reactions ( $^{238}\text{U}$ (n,n),  $^{56}\text{Fe}$ (n,n),  $^{240}\text{Pu}$ (n,n), all of them elastic scattering) for which the results are very different. However, since these results are affected by large errors, the results are compatible.

There is one instance, however, of a non-scattering reaction where the difference between TSUNAMI-3D and MCNP is significant:  $^{238}\text{U}$ (n,2n), where the TSUNAMI-3D ISC result is about four times the MCNP one. There is no MORET result for this ISC. Calculations with a higher precision have been carried out for this ISC with MCNP and have been found to produce essentially the same value, so the reason of this discrepancy remains unknown at the time of this writing. In any case, upon examination of the corresponding sensitivity profile in Annex 2, it can be observed that the sensitivity coefficient is non-zero in only two energy groups.

Concerning the sensitivity profiles presented in Annex 1, overall, the differences between the three codes are small. It can also be noticed that the sensitivity profiles obtained with MCNP and MORET are affected by much larger statistical errors than the ones obtained with TSUNAMI-3D. In the case of MORET, this can be explained by lower statistics, which also results in a higher uncertainty in the  $k_{eff}$  result listed above. However, the calculations with MCNP and TSUNAMI-3D were performed to a similar precision level in  $k_{eff}$ ; yet, the MCNP sensitivity profiles appear to be affected by much larger oscillations.

The difference between codes is especially noticeable in the case of scattering reactions, both elastic and inelastic, whose sensitivity profiles obtained with all three codes tend to have larger errors than for other reactions. A similar behaviour has been reported in [Romero 2017] for the case of the sensitivity coefficients to the elastic scattering of  $^{238}\text{U}$  and other elastic and inelastic reactions in the ALFRED reactor, to the point that we decided to perform the MCNP calculations with less than 2 pcm precision in  $k_{eff}$ .

In addition to the ISCs, the reactions with the largest contribution to the uncertainty and the value of this contribution are listed in Table 2. **Major contributors to the uncertainty in the keff of ESFR calculated with MCNP+SUMMON, TSUNAMI-3D and MORET.**

ESFR-RZ, JEFF-3.3 library, 33 energy groups								
Quantity		$\Delta k_{eff} / k_{eff}$ (%)						
		TSUNAMI-3D + SAMS	TSUNAMI-3D + SUMMON		MCNP + SUMMON		MORET + SUMMON	
		Result	Ratio	Result	Ratio	Result	Ratio	
$^{240}\text{Pu}$ (n,f)	$^{240}\text{Pu}$ (n,f)	0.582 $\pm 8.40\text{E-}05$	0.574 $\pm 4.65\text{E-}04$	0.986 $\pm 8.12\text{E-}04$	0.577 $\pm$ 2.20E-03 0.992 $\pm$ 3.78E-03	0.572 $\pm 4.41\text{E-}03$	0.983 $\pm 7.57\text{E-}03$	
$^{238}\text{U}$ (n,n')	$^{238}\text{U}$ (n,n')	0.476 $\pm 1.79\text{E-}04$	0.469 $\pm 8.36\text{E-}04$	0.985 $\pm 1.79\text{E-}03$	0.464 $\pm$ 1.35E-02 0.975 $\pm$ 2.84E-02	0.449 $\pm 1.09\text{E-}02$	0.944 $\pm 2.30\text{E-}02$	

$^{240}\text{Pu}$ (n,f)	$^{240}\text{Pu}$ (n, $\gamma$ )	-0.437 $\pm 2.02\text{E-}05$	-0.436 $\pm 2.85\text{E-}05$	0.997 $\pm 7.99\text{E-}05$	-0.438 $\pm$ 5.73E-04	1.002 $\pm$ 1.31E-03	-0.435 $\pm 3.22\text{E-}04$	0.996 $\pm 7.38\text{E-}04$
$^{239}\text{Pu}$ $\chi$	$^{239}\text{Pu}$ $\chi$	0.427 $\pm 4.17\text{E-}04$	0.428 $\pm 2.48\text{E-}03$	1.003 $\pm 5.90\text{E-}03$	0.426 $\pm$ 7.92E-03	0.997 $\pm$ 1.86E-02	---	---
$^{238}\text{U}$ (n,n')	$^{238}\text{U}$ (n,f)	-0.341 $\pm 5.51\text{E-}05$	-0.346 $\pm 2.73\text{E-}04$	1.013 $\pm 8.18\text{E-}04$	-0.345 $\pm$ 2.74E-03	1.013 $\pm$ 8.03E-03	-0.331 $\pm 3.24\text{E-}03$	0.970 $\pm 9.51\text{E-}03$
$^{239}\text{Pu}$ (n,f)	$^{239}\text{Pu}$ (n,f)	0.313 $\pm 1.21\text{E-}05$	0.313 $\pm 9.46\text{E-}05$	1.001 $\pm 3.05\text{E-}04$	0.313 $\pm$ 1.25E-03	1.000 $\pm$ 3.98E-03	0.300 $\pm 1.00\text{E-}03$	0.960 $\pm 3.21\text{E-}03$
$^{239}\text{Pu}$ $\bar{\nu}$	$^{239}\text{Pu}$ $\bar{\nu}$	0.296 $\pm 3.93\text{E-}06$	---	---	---	---	---	---
$^{238}\text{U}$ (n, $\gamma$ )	$^{238}\text{U}$ (n, $\gamma$ )	0.293 $\pm 2.73\text{E-}06$	0.293 $\pm 1.81\text{E-}05$	1.000 $\pm 1.93\text{E-}04$	0.291 $\pm$ 3.93E-04	1.006 $\pm$ 1.36E-03	0.273 $\pm 1.99\text{E-}04$	0.932 $\pm 6.78\text{E-}04$
$^{238}\text{U}$ (n,n')	$^{238}\text{U}$ (n, $\gamma$ )	0.296 $\pm 7.42\text{E-}05$	0.294 $\pm 5.66\text{E-}05$	0.992 $\pm 2.56\text{E-}04$	0.289 $\pm$ 1.31E-03	0.977 $\pm$ 4.42E-03	0.272 $\pm 6.63\text{E-}04$	0.919 $\pm 2.25\text{E-}03$
$^{240}\text{Pu}$ (n, $\gamma$ )	$^{240}\text{Pu}$ (n, $\gamma$ )	0.201 $\pm 7.20\text{E-}07$	0.202 $\pm 1.40\text{E-}05$	1.003 $\pm 6.96\text{E-}05$	0.202 $\pm$ 2.86E-04	1.007 $\pm$ 1.42E-03	0.202 $\pm 1.61\text{E-}04$	1.004 $\pm 7.99\text{E-}04$
$^{238}\text{U}$ (n,f)	$^{238}\text{U}$ (n,f)	0.192 $\pm 1.44\text{E-}05$	0.199 $\pm 1.54\text{E-}04$	1.039 $\pm 8.04\text{E-}04$	0.196 $\pm$ 3.45E-04	1.019 $\pm$ 1.80E-03	0.190 $\pm 1.81\text{E-}03$	0.989 $\pm 9.44\text{E-}03$
$^{238}\text{U}$ (n,f)	$^{238}\text{U}$ (n, $\gamma$ )	0.191 $\pm 8.33\text{E-}06$	0.195 $\pm 1.90\text{E-}05$	1.023 $\pm 1.09\text{E-}04$	0.196 $\pm$ 3.45E-04	0.976 $\pm$ 1.72E-03	0.185 $\pm 1.99\text{E-}04$	0.970 $\pm 1.04\text{E-}03$
$^{241}\text{Pu}$ $\chi$	$^{241}\text{Pu}$ $\chi$	0.166 $\pm 8.32\text{E-}05$	0.167 $\pm 1.30\text{E-}03$	1.006 $\pm 7.82\text{E-}03$	0.170 $\pm$ 3.48E-03	1.026 $\pm$ 2.10E-02	---	---
$^{239}\text{Pu}$ (n,f)	$^{239}\text{Pu}$ (n, $\gamma$ )	0.156 $\pm 1.87\text{E-}06$	0.156 $\pm 1.69\text{E-}05$	1.001 $\pm 1.98\text{E-}04$	0.156 $\pm$ 3.64E-04	1.000 $\pm$ 2.33E-03	0.153 $\pm 1.86\text{E-}04$	0.982 $\pm 1.19\text{E-}03$
$^{16}\text{O}$ (n,n)	$^{16}\text{O}$ (n,n)	0.124 $\pm 3.62\text{E-}05$	0.124 $\pm 7.98\text{E-}04$	1.002 $\pm 6.45\text{E-}03$	0.114 $\pm$ 1.08E-02	0.916 $\pm$ 8.71E-02	0.138 $\pm 8.77\text{E-}03$	1.115 $\pm 7.07\text{E-}02$
$^{238}\text{U}$ $\bar{\nu}$	$^{238}\text{U}$ $\bar{\nu}$	0.120 $\pm 3.45\text{E-}06$	---	---	---	---	---	---
$^{238}\text{U}$ (n,n)	$^{238}\text{U}$ (n,n')	-0.125 $\pm 2.00\text{E-}04$	-0.123 $\pm 2.15\text{E-}04$	0.986 $\pm 2.33\text{E-}03$	-0.146 $\pm$ 4.12E-03	1.167 $\pm$ 3.30E-02	-0.113 $\pm 2.68\text{E-}03$	0.906 $\pm 2.15\text{E-}02$
$^{239}\text{Pu}$ (n, $\gamma$ )	$^{239}\text{Pu}$ (n, $\gamma$ )	0.118 $\pm 1.19\text{E-}06$	0.118 $\pm 2.33\text{E-}05$	1.001 $\pm 1.98\text{E-}04$	0.116 $\pm$ 4.13E-04	0.981 $\pm$ 3.50E-03	0.111 $\pm 2.24\text{E-}04$	0.944 $\pm 1.90\text{E-}03$
$^{240}\text{Pu}$ (n,n')	$^{240}\text{Pu}$ (n,f)	-0.114 $\pm 2.81\text{E-}05$	-0.114 $\pm 1.18\text{E-}04$	0.998 $\pm 1.06\text{E-}03$	-0.123 $\pm$ 4.78E-04	1.075 $\pm$ 4.20E-03	-0.108 $\pm 8.33\text{E-}04$	0.950 $\pm 7.31\text{E-}03$
$^{238}\text{U}$ (n,n')	$^{238}\text{U}$ (n,2n)	-0.104 $\pm 1.18\text{E-}05$	-0.100 $\pm 3.26\text{E-}04$	0.961 $\pm 3.13\text{E-}03$	-0.050 $\pm$ 1.22E-02	0.477 $\pm$ 1.18E-01	---	---

. The values obtained with TSUNAMI-3D using its own SAMS module are used as references with which the results obtained with SUMMON and the JEFF-3.3 covariance matrices processed with NJOY21, using the sensitivity profiles obtained with MCNP, MORET and TSUNAMI-3D itself can be compared.

Two reactions are listed in the first column of Table 1, reflecting correlations between them. When the two reactions listed are the same, this means that the uncertainty is due to the covariance of a reaction cross section with itself (notice that there are correlations between the different energy groups). If two different reaction names are listed, the uncertainty is related to cross-correlations between the two reactions. In this second case, the contribution to the uncertainty can be either positive or negative. Covariances between reactions belonging to different isotopes are not included in JEFF-3.3 covariance matrices.

As was the case for the ISCs, it can be observed that the differences between the codes are rather small. The difference between TSUNAMI-3D + SAMS, TSUNAMI-3D + SUMMON and MCNP + SUMMON is usually in the order of ~1%. The discrepancy with MORET + SUMMON is somewhat larger, but still <10% (remember that MORET results have been obtained with lower statistics). The only case where the observed discrepancies are significantly larger is when scattering reactions are implied. Thus, in the case of  $^{238}\text{U}(n,n)/^{238}\text{U}(n,n')$  the difference between TSUNAMI-3D + SAMS and MCNP + SUMMON reaches ~10%. This is consistent with the observed larger uncertainties in the sensitivity coefficients of the scattering reactions. Furthermore, there is a large discrepancy between these codes (about a factor of 2) for the case of  $^{238}\text{U}(n,n')/^{238}\text{U}(n,2n)$ , but this was somewhat expected given the large discrepancy in the  $^{238}\text{U}(n,2n)$  sensitivity profile.

As a final comment, total uncertainty results in  $k_{eff}$  are not provided because the purpose of this work is the cross comparison between codes and not the results themselves. Furthermore, it is obvious that for the total uncertainty results to be consistently compared, the same reactions would have to be considered in all the codes, which was not the case here.

## 4.2. Sodium void reactivity worth

The second integral quantity for which S/U have been calculated and intercompared is the sodium void reactivity worth. This quantity was not calculated with MORET, since this code is not capable of performing sensitivity calculations to eigenvalue differences, therefore only the results obtained with TSUNAMI-3D and MCNP are presented in this section.

The case analysed corresponds to the voiding of the fissile core (both the inner and outer regions) and the plenum above them (Figure 3). This is labelled as “void 5” in [Davies 2020]. The values of reactivity worth obtained with MCNP and KENO are:

$$\rho_{Void,MCNP} = 1191 \pm 11 pcm$$

$$\rho_{Void,KENO} = 1230 \pm 12 pcm$$

It is worth mentioning that these results are different from the ones published in [Davies 2020], where a sodium voiding worth of 251 pcm was obtained with KENO and JEFF-3.1 for the full 3D heterogeneous model. The main reason for this discrepancy is the use here of a simplified RZ model instead of a full 3D model (among other things, the voiding scenario is not completely equivalent as in the full 3D heterogeneous model, the sodium outside wrapper was not voided). On the other hand, the result also differs with respect to the one published in [Romojaro 2021], where a void worth of 989 pcm was obtained with KENO and JEFF-3.1 for the RZ model. The discrepancy in this case is due to the use of a different nuclear data library (JEFF-3.3 instead of JEFF-3.1). Although the difference in the results would be worth investigating, this was not done as it was considered beyond the purpose of our study.

ISCs for the sodium void reactivity worth for the most relevant reactions are presented in Table 3. **Reactions with the largest Integrated Sensitivity Coefficients for the sodium void worth of ESFR.**

ESFR-RZ -33 energy groups	
Reaction	Sensitivity ( $\rho_{Void}$ ) - Integrated values

	TSUNAMI-3D	MCNP	
		Result	Ratio
<sup>239</sup> Pu (n,f)	-1.009E+00 ± 8.485E-03	-1.059E+00 ± 1.689E-01	1.05 ± 0.17
<sup>238</sup> U (n,γ)	7.839E-01 ± 3.720E-03	8.486E-01 ± 3.835E-02	1.08 ± 0.05
<sup>23</sup> Na (n,n)	6.412E-01 ± 5.834E-02	5.096E-01 ± 9.580E-02*	0.79 ± 0.17
<sup>239</sup> Pu (n,γ)	4.544E-01 ± 1.136E-03	4.624E-01 ± 1.209E-02	1.02 ± 0.03
<sup>238</sup> U (n,n')	-2.972E-01 ± 1.447E-02	-2.907E-01 ± 5.410E-02*	0.98 ± 0.19
<sup>240</sup> Pu (n,γ)	1.834E-01 ± 5.709E-04	1.872E-01 ± 6.724E-03	1.02 ± 0.04
<sup>238</sup> U (n,n)	2.934E-01 ± 9.789E-02	1.855E-01 ± 1.586E-01*	0.63 ± 0.58
<sup>240</sup> Pu (n,f)	1.529E-01 ± 4.633E-03	1.656E-01 ± 2.839E-02	1.08 ± 0.19
<sup>238</sup> U (n,f)	1.538E-01 ± 5.925E-03	1.504E-01 ± 6.372E-02	0.98 ± 0.42
<sup>54</sup> Fe (n,n)	8.468E-02 ± 1.632E-02	8.344E-02 ± 4.866E-02*	0.99 ± 0.61
<sup>23</sup> Na (n,γ)	8.177E-02 ± 6.161E-05	8.289E-02 ± 8.639E-04	1.01 ± 0.01
<sup>56</sup> Fe (n,γ)	8.559E-02 ± 6.198E-04	7.664E-02 ± 9.471E-03	0.90 ± 0.11
<sup>241</sup> Pu (n,γ)	3.058E-02 ± 1.006E-04	3.323E-02 ± 1.072E-03	1.09 ± 0.04
<sup>238</sup> Pu (n,γ)	2.235E-02 ± 7.150E-05	2.467E-02 ± 8.391E-04	1.10 ± 0.04
<sup>56</sup> Fe (n,n)	5.335E-01 ± 1.136E-01	2.243E-02 ± 5.149E-01*	0.04 ± 0.97
<sup>240</sup> Pu (n,n)	3.458E-02 ± 1.009E-02	2.135E-02 ± 3.986E-02*	0.62 ± 1.17
<sup>151</sup> Sm (n,γ)	1.534E-02 ± 3.771E-05	1.575E-02 ± 3.957E-04	1.03 ± 0.03
<sup>240</sup> Pu (n,n')	-1.006E-02 ± 2.565E-03	-1.144E-02 ± 1.244E-02*	1.14 ± 1.27
<sup>137</sup> Cs (n,n)	-4.214E-03 ± 2.164E-03	1.046E-02 ± 9.661E-03	-2.48 ± 2.62
<sup>239</sup> Pu (n,n')	-1.678E-02 ± 3.045E-03	-8.939E-03 ± 1.443E-02*	0.53 ± 0.87
<sup>133</sup> Cs (n,n)	4.453E-04 ± 1.870E-03	7.921E-03 ± 8.837E-03*	17.79 ± 77.29
<sup>151</sup> Sm (n,n)	3.642E-04 ± 6.185E-04	5.180E-03 ± 3.156E-03*	14.22 ± 25.66
<sup>134</sup> Xe (n,n)	1.711E-03 ± 2.178E-03	4.557E-03 ± 1.002E-02*	2.66 ± 6.77
<sup>141</sup> Pr (n,n)	2.106E-03 ± 1.880E-03	-2.652E-03 ± 8.913E-03*	-1.26 ± 4.38
<sup>104</sup> Ru (n,n)	1.894E-03 ± 2.247E-03	2.194E-03 ± 9.943E-03*	1.16 ± 5.43
<sup>147</sup> Sm (n,n)	-7.888E-05 ± 7.395E-04	-1.928E-03 ± 3.639E-03*	24.44 ± 233.69
<sup>238</sup> Pu (n,n')	-5.469E-05 ± 6.378E-04	1.610E-03 ± 3.003E-03*	-29.44 ± 347.72
<sup>239</sup> Pu (n,n)	3.389E-02 ± 1.121E-02	2.485E-04 ± 4.786E-02*	0.01 ± 1.41

\*NOTE: In the case of MCNP, the results calculated with 2 pcm in  $k_{eff}$  (~2.8 pcm in  $\rho_{Void}$ ) for the case of scattering (elastic and inelastic) reactions and 8 pcm (~11 pcm in  $\rho_{Void}$ ) for all other reactions.

and sensitivity profiles for all these reactions are presented in Annex 2. Overall, the agreement between codes is rather good, although in this case the statistical uncertainty in the results is noticeably larger than in the case of  $k_{eff}$  (~10% for reactions other than scattering). This can be explained because sodium void effect calculations involve the evaluation of relatively small differences between similar values (in this case, the reactivity values of the reference and the voided states), and hence more calculations would be required than for the  $k_{eff}$  S/U analyses for the same final statistical uncertainty. As in the case for  $k_{eff}$ , the largest uncertainties are observed for scattering reactions. This is despite the fact that the ISCs for all scattering (elastic and inelastic) reactions have been calculated with a fairly-tight 2 pcm precision in  $k_{eff}$  (or about 2.8 pcm precision in  $\rho_{Void}$ )

The uncertainty results are presented in Table 4. **Major contributors to the uncertainty in the sodium void scenario of ESRF calculated with MCNP+SUMMON and TSUNAMI-3D.**

ESFR-RZ (sodium-void-scenario), JEFF-3.3 library, 33 groups					
Quantity	$\Delta\rho / \rho$ (%)				
	TSUNAMI-3D +TSAR	TSUNAMI-3D + SUMMON		MCNP + SUMMON	
		Result	Ratio	Result	Ratio

$^{239}\text{Pu}(n,f)$	$^{239}\text{Pu}(n,f)$	5.086 $\pm 5.32\text{E-}03$	5.085 $\pm 1.31\text{E-}02$	1.0000 $\pm 0.0028$	5.489 $\pm 1.86\text{E-}01$	1.0792 $\pm 0.0365$
$^{239}\text{Pu}(n,\gamma)$	$^{239}\text{Pu}(n,\gamma)$	2.406 $\pm 6.02\text{E-}04$	2.406 $\pm 3.39\text{E-}03$	0.9998 $\pm 0.0014$	2.443 $\pm 6.49\text{E-}02$	1.0154 $\pm 0.0270$
$^{238}\text{U}(n,n')$	$^{238}\text{U}(n,n')$	1.911 $\pm 1.19\text{E-}02$	1.871 $\pm 9.61\text{E-}02$	0.9790 $\pm 0.0507$	1.802 $\pm 3.91\text{E-}01^*$	0.9431 $\pm 0.2045$
$^{23}\text{Na}(n,n)$	$^{23}\text{Na}(n,n)$	1.843 $\pm 9.12\text{E-}03$	1.840 $\pm 7.33\text{E-}02$	0.9985 $\pm 0.0401$	1.535 $\pm 2.54\text{E-}01^*$	0.8330 $\pm 0.1381$
$^{239}\text{Pu}(n,f)$	$^{239}\text{Pu}(n,\gamma)$	-1.781 $\pm 5.31\text{E-}04$	-1.781 $\pm 2.16\text{E-}03$	0.9998 $\pm 0.0012$	-1.857 $\pm 4.61\text{E-}02$	1.0428 $\pm 0.0259$
$^{238}\text{U}(n,\gamma)$	$^{238}\text{U}(n,\gamma)$	1.721 $\pm 4.13\text{E-}04$	1.717 $\pm 2.53\text{E-}03$	0.9979 $\pm 0.0015$	1.762 $\pm 5.35\text{E-}02$	1.0239 $\pm 0.0311$
$^{238}\text{U}(n,n')$	$^{238}\text{U}(n,\gamma)$	-1.623 $\pm 6.78\text{E-}03$	-1.589 $\pm 4.82\text{E-}03$	0.9793 $\pm 0.0051$	-1.886 $\pm 1.22\text{E-}01$	1.1622 $\pm 0.0755$
$^{238}\text{U}(n,n)$	$^{238}\text{U}(n,n')$	-1.547 $\pm 1.37\text{E-}02$	-1.519 $\pm 7.61\text{E-}02$	0.9822 $\pm 0.0499$	-1.050 $\pm 2.24\text{E-}01^*$	0.6791 $\pm 0.1446$
$^{241}\text{Pu}(n,f)$	$^{241}\text{Pu}(n,f)$	1.369 $\pm 1.74\text{E-}03$	1.367 $\pm 1.18\text{E-}02$	0.9987 $\pm 0.0087$	1.457 $\pm 8.82\text{E-}02$	1.0643 $\pm 0.0644$
$^{23}\text{Na}(n,n')$	$^{23}\text{Na}(n,n')$	1.330 $\pm 9.20\text{E-}04$	1.316 $\pm 8.52\text{E-}03$	0.9893 $\pm 0.0064$	1.309 $\pm 3.33\text{E-}02^*$	0.9844 $\pm 0.0251$
$^{23}\text{Na}(n,\gamma)$	$^{23}\text{Na}(n,\gamma)$	1.316 $\pm 8.16\text{E-}05$	1.910 $\pm 1.38\text{E-}03$	1.4516 $\pm 0.0011$	1.984 $\pm 2.83\text{E-}02$	1.5076 $\pm 0.0215$
$^{56}\text{Fe}(n,n)$	$^{56}\text{Fe}(n,n)$	1.274 $\pm 1.28\text{E-}02$	1.274 $\pm 1.15\text{E-}01$	1.0000 $\pm 0.0911$	1.181 $\pm 2.65\text{E-}01^*$	0.9272 $\pm 0.2082$
$^{238}\text{U}(n,n')$	$^{238}\text{U}(n,f)$	-1.044 $\pm 2.82\text{E-}03$	-1.055 $\pm 4.25\text{E-}02$	1.0106 $\pm 0.0408$	-1.111 $\pm 4.74\text{E-}01$	1.0639 $\pm 0.4541$
$^{238}\text{U}(n,n)$	$^{238}\text{U}(n,\gamma)$	0.983 $\pm 5.39\text{E-}03$	0.971 $\pm 2.15\text{E-}03$	0.9882 $\pm 0.0058$	0.970 $\pm 4.04\text{E-}01$	0.9872 $\pm 0.4111$
$^{240}\text{Pu}(n,f)$	$^{240}\text{Pu}(n,f)$	0.953 $\pm 9.54\text{E-}03$	0.925 $\pm 5.12\text{E-}02$	0.9708 $\pm 0.0546$	0.948 $\pm 2.58\text{E-}01$	0.9948 $\pm 0.2704$
$^{56}\text{Fe}(n,\gamma)$	$^{56}\text{Fe}(n,\gamma)$	0.773 $\pm 4.40\text{E-}04$	0.773 $\pm 4.49\text{E-}03$	0.9994 $\pm 0.0058$	0.736 $\pm 8.20\text{E-}02$	0.9525 $\pm 0.1061$
$^{238}\text{U}(n,n)$	$^{238}\text{U}(n,f)$	0.745 $\pm 3.93\text{E-}03$	0.759 $\pm 2.99\text{E-}02$	1.0187 $\pm 0.0405$	0.970 $\pm 4.04\text{E-}01$	1.3026 $\pm 0.5424$
$^{240}\text{Pu}(n,f)$	$^{240}\text{Pu}(n,\gamma)$	0.697 $\pm 2.81\text{E-}03$	0.687 $\pm 3.26\text{E-}03$	0.9852 $\pm 0.0061$	0.727 $\pm 6.65\text{E-}02$	1.0425 $\pm 0.0955$
$^{238}\text{U}(n,n)$	$^{238}\text{U}(n,n)$	0.694 $\pm 4.05\text{E-}03$	0.685 $\pm 1.11\text{E-}01$	0.9877 $\pm 0.1608$	0.381 $\pm 3.59\text{E-}01^*$	0.5488 $\pm 0.5174$

\*Results calculated with 2 pcm in keff (~2.8 pcm in pvoid) instead 8 pcm (~11 pcm in pvoid).

. The discrepancies between the codes are in this case larger than in Section 4.1, in the range of 1-10% for the individual reactions, reaching up to ~50%. Again, as in the case of the uncertainty in  $k_{eff}$  in Section 4.1, it can be observed that the individual reactions having the largest discrepancies involve scattering, the only notable exception being  $^{23}\text{Na} (n,\gamma)$ . However, in this case it has been found that, when the TSUNAMI-3D sensitivity profiles are used within SUMMON with the covariance matrices processed with NJOY21, the result obtained is much closer to the result obtained with MCNP (KSEN) + SUMMON than to the result obtained with TSUNAMI-3D + TSAR, suggesting that the reason for the discrepancy is in the covariance matrices rather than in the sensitivity coefficients. Further research is required to clarify this.

As a final result, in order to better understand the impact of the precision (statistics) on the uncertainty results obtained with MCNP + SUMMON, the values of the uncertainty in  $\rho_{Void}$  due to the  $^{23}\text{Na}$  and  $^{238}\text{U}$  elastic scattering calculated with increasing precision levels (i.e. increasing statistics) are plotted in Figure 4. The variations in the  $\Delta\rho/\rho$  result with the statistics are very apparent, but comparable with the statistical errors (error bars) in  $\Delta\rho/\rho$  provided by the SUMMON code.

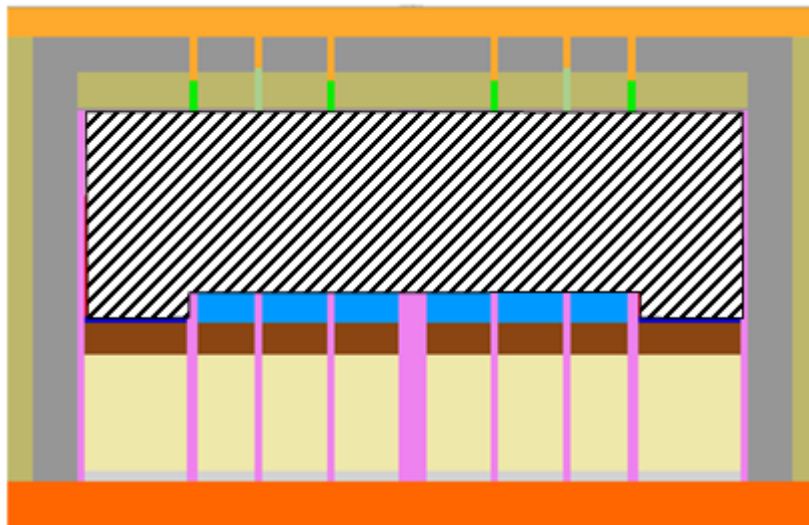


Figure 3. Regions voided of sodium.

**Table 1. Reactions with the largest Integrated Sensitivity Coefficients for the  $k_{eff}$  of ESFR.**

ESFR-RZ -33 energy groups					
Sensitivity ( $k_{eff}$ ) - Integrated sensitivity values					
Reaction	TSUNAMI-3D	MCNP		MORET	
		Result	Ratio	Result	Ratio
$^{239}\text{Pu}$ (n,f)	4.776E-01 $\pm$ 7.331E-05	4.777E-01 $\pm$ 1.452E-03	1.000 $\pm$ 0.003	4.628E-01 $\pm$ 1.414E-03	0.969 $\pm$ 0.003
$^{238}\text{U}$ (n, $\gamma$ )	-1.932E-01 $\pm$ 3.297E-05	-1.912E-01 $\pm$ 3.293E-04	0.990 $\pm$ 0.002	-1.776E-01 $\pm$ 1.795E-04	0.919 $\pm$ 0.001
$^{241}\text{Pu}$ (n,f)	7.759E-02 $\pm$ 4.224E-05	7.789E-02 $\pm$ 2.681E-04	1.004 $\pm$ 0.003	7.648E-02 $\pm$ 5.840E-04	0.986 $\pm$ 0.008
$^{238}\text{U}$ (n,f)	7.513E-02 $\pm$ 4.972E-05	7.518E-02 $\pm$ 5.206E-04	1.001 $\pm$ 0.007	7.123E-02 $\pm$ 6.180E-04	0.948 $\pm$ 0.008
$^{238}\text{U}$ (n,n')	-7.151E-02 $\pm$ 1.252E-04	-6.957E-02 $\pm$ 1.909E-03	0.973 $\pm$ 0.027	-6.775E-02 $\pm$ 1.542E-03	0.947 $\pm$ 0.022
$^{16}\text{O}$ (n,n)	-6.270E-02 $\pm$ 7.738E-04	-5.746E-02 $\pm$ 5.513E-03	0.916 $\pm$ 0.089	-6.861E-02 $\pm$ 4.489E-03	1.094 $\pm$ 0.080
$^{240}\text{Pu}$ (n,f)	5.591E-02 $\pm$ 4.022E-05	5.624E-02 $\pm$ 2.359E-04	1.006 $\pm$ 0.004	5.594E-02 $\pm$ 4.995E-04	1.001 $\pm$ 0.009
$^{239}\text{Pu}$ (n, $\gamma$ )	-4.018E-02 $\pm$ 1.070E-05	-3.958E-02 $\pm$ 1.060E-04	0.985 $\pm$ 0.003	-3.824E-02 $\pm$ 5.918E-05	0.952 $\pm$ 0.001
$^{240}\text{Pu}$ (n, $\gamma$ )	-2.487E-02 $\pm$ 5.360E-06	-2.486E-02 $\pm$ 6.045E-05	1.000 $\pm$ 0.002	-2.482E-02 $\pm$ 3.810E-05	0.998 $\pm$ 0.002
$^{56}\text{Fe}$ (n,n')	-2.136E-02 $\pm$ 5.696E-05	-2.120E-02 $\pm$ 8.179E-04	0.992 $\pm$ 0.038	-2.016E-02 $\pm$ 6.475E-04	0.944 $\pm$ 0.030
$^{238}\text{U}$ (n,n)	1.114E-05 $\pm$ 2.079E-05	1.427E-02 $\pm$ 5.412E-03	1281 $\pm$ 2439	1.216E-02 $\pm$ 4.463E-03	1091 $\pm$ 2075
$^{56}\text{Fe}$ (n, $\gamma$ )	-1.015E-02 $\pm$ 5.737E-06	-9.466E-03 $\pm$ 8.767E-05	0.933 $\pm$ 0.009	-7.324E-03 $\pm$ 5.829E-05	0.722 $\pm$ 0.006
$^{241}\text{Pu}$ (n, $\gamma$ )	-4.341E-03 $\pm$ 9.355E-07	-4.353E-03 $\pm$ 9.775E-06	1.003 $\pm$ 0.002	-4.344E-03 $\pm$ 5.446E-06	1.001 $\pm$ 0.001
$^{240}\text{Pu}$ (n,n')	-2.646E-03 $\pm$ 2.225E-05	-2.566E-03 $\pm$ 3.982E-04	0.970 $\pm$ 0.151	-2.681E-03 $\pm$ 3.423E-04	1.013 $\pm$ 0.130
$^{238}\text{Pu}$ (n, $\gamma$ )	-2.485E-03 $\pm$ 6.633E-07	-2.496E-03 $\pm$ 7.946E-06	1.005 $\pm$ 0.003	-2.494E-03 $\pm$ 5.584E-06	1.004 $\pm$ 0.002
$^{239}\text{Pu}$ (n,n')	-3.288E-03 $\pm$ 2.640E-05	-2.424E-03 $\pm$ 4.799E-04	0.737 $\pm$ 0.146	-2.825E-03 $\pm$ 4.154E-04	0.859 $\pm$ 0.127
$^{56}\text{Fe}$ (n,n)	-2.139E-04 $\pm$ 9.937E-04	1.601E-03 $\pm$ 4.626E-03	-7.5 $\pm$ 41	-1.060E-02 $\pm$ 3.475E-03	50 $\pm$ 231
$^{23}\text{Na}$ (n, $\gamma$ )	-1.513E-03 $\pm$ 6.426E-07	-1.426E-03 $\pm$ 7.471E-06	0.943 $\pm$ 0.005	-8.508E-04 $\pm$ 3.005E-06	0.562 $\pm$ 0.002
$^{240}\text{Pu}$ (n,n)	4.934E-04 $\pm$ 8.649E-05	1.147E-03 $\pm$ 1.460E-03	2.3 $\pm$ 3.0	-5.575E-04 $\pm$ 1.172E-03	-1.13 $\pm$ 2.38
$^{104}\text{Ru}$ (n, $\gamma$ )	-5.875E-04 $\pm$ 1.983E-07	-5.855E-04 $\pm$ 3.372E-06	0.997 $\pm$ 0.006	-5.729E-04 $\pm$ 2.357E-06	0.975 $\pm$ 0.004
$^{238}\text{U}$ (n,2n)	1.702E-03 $\pm$ 5.597E-06	4.234E-04 $\pm$ 1.052E-04 <sup>2</sup>	0.249 $\pm$ 0.062	---	---

<sup>2</sup>  $^{238}\text{U}$  (n,2n) ISC calculated with MCNP with a precision of 2 pcm in  $k_{eff}$  is  $4.284637\text{E-}04 \pm 2.706370\text{E-}05$ .

**Table 2. Major contributors to the uncertainty in the  $k_{eff}$  of ESRF calculated with MCNP+SUMMON, TSUNAMI-3D and MORET.**

		ESFR-RZ, JEFF-3.3 library, 33 energy groups						
		$\Delta k_{eff} / k_{eff}$ (%)						
Quantity		TSUNAMI-3D + SAMS	TSUNAMI-3D + SUMMON		MCNP + SUMMON		MORET + SUMMON	
			Result	Ratio	Result	Ratio	Result	Ratio
$^{240}\text{Pu}$ (n,f)	$^{240}\text{Pu}$ (n,f)	0.582 $\pm 8.40\text{E-}05$	0.574 $\pm 4.65\text{E-}04$	0.986 $\pm 8.12\text{E-}04$	0.577 $\pm$ 2.20E-03	0.992 $\pm$ 3.78E-03	0.572 $\pm 4.41\text{E-}03$	0.983 $\pm 7.57\text{E-}03$
$^{238}\text{U}$ (n,n')	$^{238}\text{U}$ (n,n')	0.476 $\pm 1.79\text{E-}04$	0.469 $\pm 8.36\text{E-}04$	0.985 $\pm 1.79\text{E-}03$	0.464 $\pm$ 1.35E-02	0.975 $\pm$ 2.84E-02	0.449 $\pm 1.09\text{E-}02$	0.944 $\pm 2.30\text{E-}02$
$^{240}\text{Pu}$ (n,f)	$^{240}\text{Pu}$ (n, $\gamma$ )	-0.437 $\pm 2.02\text{E-}05$	-0.436 $\pm 2.85\text{E-}05$	0.997 $\pm 7.99\text{E-}05$	-0.438 $\pm$ 5.73E-04	1.002 $\pm$ 1.31E-03	-0.435 $\pm 3.22\text{E-}04$	0.996 $\pm 7.38\text{E-}04$
$^{239}\text{Pu}$ $\chi$	$^{239}\text{Pu}$ $\chi$	0.427 $\pm 4.17\text{E-}04$	0.428 $\pm 2.48\text{E-}03$	1.003 $\pm 5.90\text{E-}03$	0.426 $\pm$ 7.92E-03	0.997 $\pm$ 1.86E-02	---	---
$^{238}\text{U}$ (n,n')	$^{238}\text{U}$ (n,f)	-0.341 $\pm 5.51\text{E-}05$	-0.346 $\pm 2.73\text{E-}04$	1.013 $\pm 8.18\text{E-}04$	-0.345 $\pm$ 2.74E-03	1.013 $\pm$ 8.03E-03	-0.331 $\pm 3.24\text{E-}03$	0.970 $\pm 9.51\text{E-}03$
$^{239}\text{Pu}$ (n,f)	$^{239}\text{Pu}$ (n,f)	0.313 $\pm 1.21\text{E-}05$	0.313 $\pm 9.46\text{E-}05$	1.001 $\pm 3.05\text{E-}04$	0.313 $\pm$ 1.25E-03	1.000 $\pm$ 3.98E-03	0.300 $\pm 1.00\text{E-}03$	0.960 $\pm 3.21\text{E-}03$
$^{239}\text{Pu}$ $\bar{\nu}$	$^{239}\text{Pu}$ $\bar{\nu}$	0.296 $\pm 3.93\text{E-}06$	---	---	---	---	---	---
$^{238}\text{U}$ (n, $\gamma$ )	$^{238}\text{U}$ (n, $\gamma$ )	0.293 $\pm 2.73\text{E-}06$	0.293 $\pm 1.81\text{E-}05$	1.000 $\pm 1.93\text{E-}04$	0.291 $\pm$ 3.93E-04	1.006 $\pm$ 1.36E-03	0.273 $\pm 1.99\text{E-}04$	0.932 $\pm 6.78\text{E-}04$
$^{238}\text{U}$ (n,n')	$^{238}\text{U}$ (n, $\gamma$ )	0.296 $\pm 7.42\text{E-}05$	0.294 $\pm 5.66\text{E-}05$	0.992 $\pm 2.56\text{E-}04$	0.289 $\pm$ 1.31E-03	0.977 $\pm$ 4.42E-03	0.272 $\pm 6.63\text{E-}04$	0.919 $\pm 2.25\text{E-}03$
$^{240}\text{Pu}$ (n, $\gamma$ )	$^{240}\text{Pu}$ (n, $\gamma$ )	0.201 $\pm 7.20\text{E-}07$	0.202 $\pm 1.40\text{E-}05$	1.003 $\pm 6.96\text{E-}05$	0.202 $\pm$ 2.86E-04	1.007 $\pm$ 1.42E-03	0.202 $\pm 1.61\text{E-}04$	1.004 $\pm 7.99\text{E-}04$
$^{238}\text{U}$ (n,f)	$^{238}\text{U}$ (n,f)	0.192 $\pm 1.44\text{E-}05$	0.199 $\pm 1.54\text{E-}04$	1.039 $\pm 8.04\text{E-}04$	0.196 $\pm$ 3.45E-04	1.019 $\pm$ 1.80E-03	0.190 $\pm 1.81\text{E-}03$	0.989 $\pm 9.44\text{E-}03$
$^{238}\text{U}$ (n,f)	$^{238}\text{U}$ (n, $\gamma$ )	0.191 $\pm 8.33\text{E-}06$	0.195 $\pm 1.90\text{E-}05$	1.023 $\pm 1.09\text{E-}04$	0.196 $\pm$ 3.45E-04	0.976 $\pm$ 1.72E-03	0.185 $\pm 1.99\text{E-}04$	0.970 $\pm 1.04\text{E-}03$
$^{241}\text{Pu}$ $\chi$	$^{241}\text{Pu}$ $\chi$	0.166 $\pm 8.32\text{E-}05$	0.167 $\pm 1.30\text{E-}03$	1.006 $\pm 7.82\text{E-}03$	0.170 $\pm$ 3.48E-03	1.026 $\pm$ 2.10E-02	---	---
$^{239}\text{Pu}$ (n,f)	$^{239}\text{Pu}$ (n, $\gamma$ )	0.156 $\pm 1.87\text{E-}06$	0.156 $\pm 1.69\text{E-}05$	1.001 $\pm 1.98\text{E-}04$	0.156 $\pm$ 3.64E-04	1.000 $\pm$ 2.33E-03	0.153 $\pm 1.86\text{E-}04$	0.982 $\pm 1.19\text{E-}03$
$^{16}\text{O}$ (n,n)	$^{16}\text{O}$ (n,n)	0.124 $\pm 3.62\text{E-}05$	0.124 $\pm 7.98\text{E-}04$	1.002 $\pm 6.45\text{E-}03$	0.114 $\pm$ 1.08E-02	0.916 $\pm$ 8.71E-02	0.138 $\pm 8.77\text{E-}03$	1.115 $\pm 7.07\text{E-}02$
$^{238}\text{U}$ $\bar{\nu}$	$^{238}\text{U}$ $\bar{\nu}$	0.120 $\pm 3.45\text{E-}06$	---	---	---	---	---	---
$^{238}\text{U}$ (n,n)	$^{238}\text{U}$ (n,n')	-0.125 $\pm 2.00\text{E-}04$	-0.123 $\pm 2.15\text{E-}04$	0.986 $\pm 2.33\text{E-}03$	-0.146 $\pm$ 4.12E-03	1.167 $\pm$ 3.30E-02	-0.113 $\pm 2.68\text{E-}03$	0.906 $\pm 2.15\text{E-}02$
$^{239}\text{Pu}$ (n, $\gamma$ )	$^{239}\text{Pu}$ (n, $\gamma$ )	0.118 $\pm 1.19\text{E-}06$	0.118 $\pm 2.33\text{E-}05$	1.001 $\pm 1.98\text{E-}04$	0.116 $\pm$ 4.13E-04	0.981 $\pm$ 3.50E-03	0.111 $\pm 2.24\text{E-}04$	0.944 $\pm 1.90\text{E-}03$
$^{240}\text{Pu}$ (n,n')	$^{240}\text{Pu}$ (n,f)	-0.114 $\pm 2.81\text{E-}05$	-0.114 $\pm 1.18\text{E-}04$	0.998 $\pm 1.06\text{E-}03$	-0.123 $\pm$ 4.78E-04	1.075 $\pm$ 4.20E-03	-0.108 $\pm 8.33\text{E-}04$	0.950 $\pm 7.31\text{E-}03$
$^{238}\text{U}$ (n,n')	$^{238}\text{U}$ (n,2n)	-0.104 $\pm 1.18\text{E-}05$	-0.100 $\pm 3.26\text{E-}04$	0.961 $\pm 3.13\text{E-}03$	-0.050 $\pm$ 1.22E-02	0.477 $\pm$ 1.18E-01	---	---

**Table 3. Reactions with the largest Integrated Sensitivity Coefficients for the sodium void worth of ESFR.**

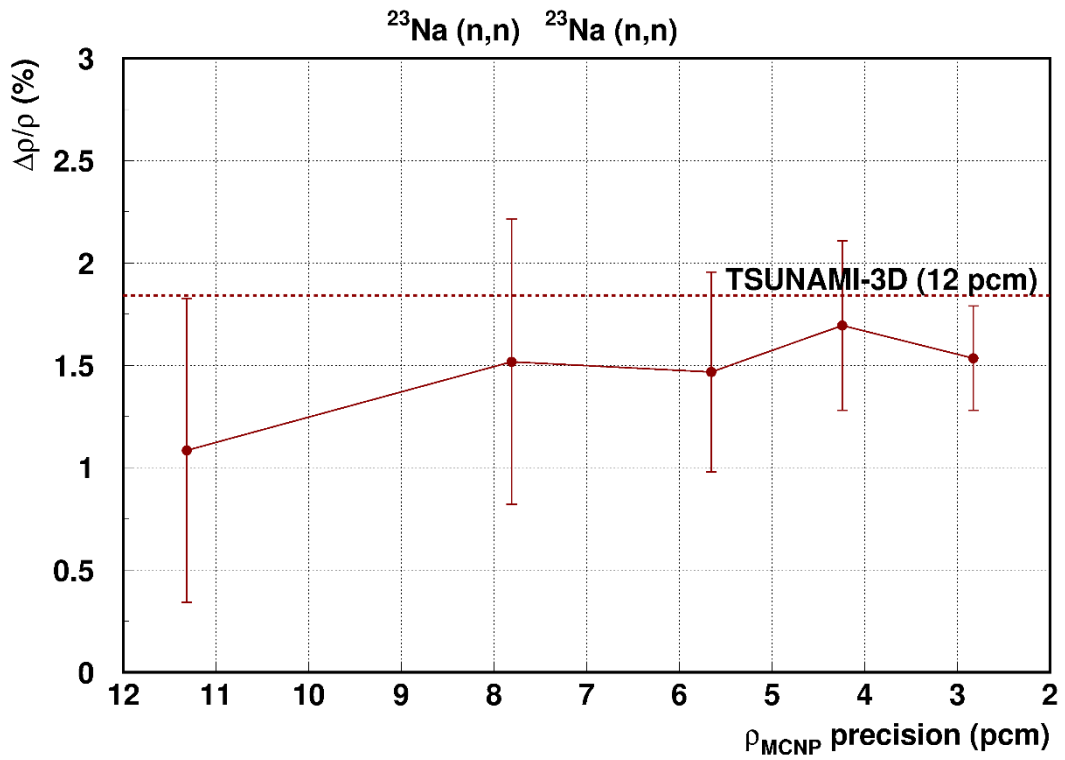
ESFR-RZ -33 energy groups			
Reaction	Sensitivity ( $\rho_{void}$ ) - Integrated values		
	TSUNAMI-3D	MCNP	
		Result	Ratio
<sup>239</sup> Pu (n,f)	-1.009E+00 ± 8.485E-03	-1.059E+00 ± 1.689E-01	1.05 ± 0.17
<sup>238</sup> U (n,γ)	7.839E-01 ± 3.720E-03	8.486E-01 ± 3.835E-02	1.08 ± 0.05
<sup>23</sup> Na (n,n)	6.412E-01 ± 5.834E-02	5.096E-01 ± 9.580E-02*	0.79 ± 0.17
<sup>239</sup> Pu (n,γ)	4.544E-01 ± 1.136E-03	4.624E-01 ± 1.209E-02	1.02 ± 0.03
<sup>238</sup> U (n,n')	-2.972E-01 ± 1.447E-02	-2.907E-01 ± 5.410E-02*	0.98 ± 0.19
<sup>240</sup> Pu (n,γ)	1.834E-01 ± 5.709E-04	1.872E-01 ± 6.724E-03	1.02 ± 0.04
<sup>238</sup> U (n,n)	2.934E-01 ± 9.789E-02	1.855E-01 ± 1.586E-01*	0.63 ± 0.58
<sup>240</sup> Pu (n,f)	1.529E-01 ± 4.633E-03	1.656E-01 ± 2.839E-02	1.08 ± 0.19
<sup>238</sup> U (n,f)	1.538E-01 ± 5.925E-03	1.504E-01 ± 6.372E-02	0.98 ± 0.42
<sup>54</sup> Fe (n,n)	8.468E-02 ± 1.632E-02	8.344E-02 ± 4.866E-02*	0.99 ± 0.61
<sup>23</sup> Na (n,γ)	8.177E-02 ± 6.161E-05	8.289E-02 ± 8.639E-04	1.01 ± 0.01
<sup>56</sup> Fe (n,γ)	8.559E-02 ± 6.198E-04	7.664E-02 ± 9.471E-03	0.90 ± 0.11
<sup>241</sup> Pu (n,γ)	3.058E-02 ± 1.006E-04	3.323E-02 ± 1.072E-03	1.09 ± 0.04
<sup>238</sup> Pu (n,γ)	2.235E-02 ± 7.150E-05	2.467E-02 ± 8.391E-04	1.10 ± 0.04
<sup>56</sup> Fe (n,n)	5.335E-01 ± 1.136E-01	2.243E-02 ± 5.149E-01*	0.04 ± 0.97
<sup>240</sup> Pu (n,n)	3.458E-02 ± 1.009E-02	2.135E-02 ± 3.986E-02*	0.62 ± 1.17
<sup>151</sup> Sm (n,γ)	1.534E-02 ± 3.771E-05	1.575E-02 ± 3.957E-04	1.03 ± 0.03
<sup>240</sup> Pu (n,n')	-1.006E-02 ± 2.565E-03	-1.144E-02 ± 1.244E-02*	1.14 ± 1.27
<sup>137</sup> Cs (n,n)	-4.214E-03 ± 2.164E-03	1.046E-02 ± 9.661E-03	-2.48 ± 2.62
<sup>239</sup> Pu (n,n')	-1.678E-02 ± 3.045E-03	-8.939E-03 ± 1.443E-02*	0.53 ± 0.87
<sup>133</sup> Cs (n,n)	4.453E-04 ± 1.870E-03	7.921E-03 ± 8.837E-03*	17.79 ± 77.29
<sup>151</sup> Sm (n,n)	3.642E-04 ± 6.185E-04	5.180E-03 ± 3.156E-03*	14.22 ± 25.66
<sup>134</sup> Xe (n,n)	1.711E-03 ± 2.178E-03	4.557E-03 ± 1.002E-02*	2.66 ± 6.77
<sup>141</sup> Pr (n,n)	2.106E-03 ± 1.880E-03	-2.652E-03 ± 8.913E-03*	-1.26 ± 4.38
<sup>104</sup> Ru (n,n)	1.894E-03 ± 2.247E-03	2.194E-03 ± 9.943E-03*	1.16 ± 5.43
<sup>147</sup> Sm (n,n)	-7.888E-05 ± 7.395E-04	-1.928E-03 ± 3.639E-03*	24.44 ± 233.69
<sup>238</sup> Pu (n,n')	-5.469E-05 ± 6.378E-04	1.610E-03 ± 3.003E-03*	-29.44 ± 347.72
<sup>239</sup> Pu (n,n)	3.389E-02 ± 1.121E-02	2.485E-04 ± 4.786E-02*	0.01 ± 1.41

\*NOTE: In the case of MCNP, the results calculated with 2 pcm in  $k_{eff}$  (~2.8 pcm in  $\rho_{void}$ ) for the case of scattering (elastic and inelastic) reactions and 8 pcm (~11 pcm in  $\rho_{void}$ ) for all other reactions.

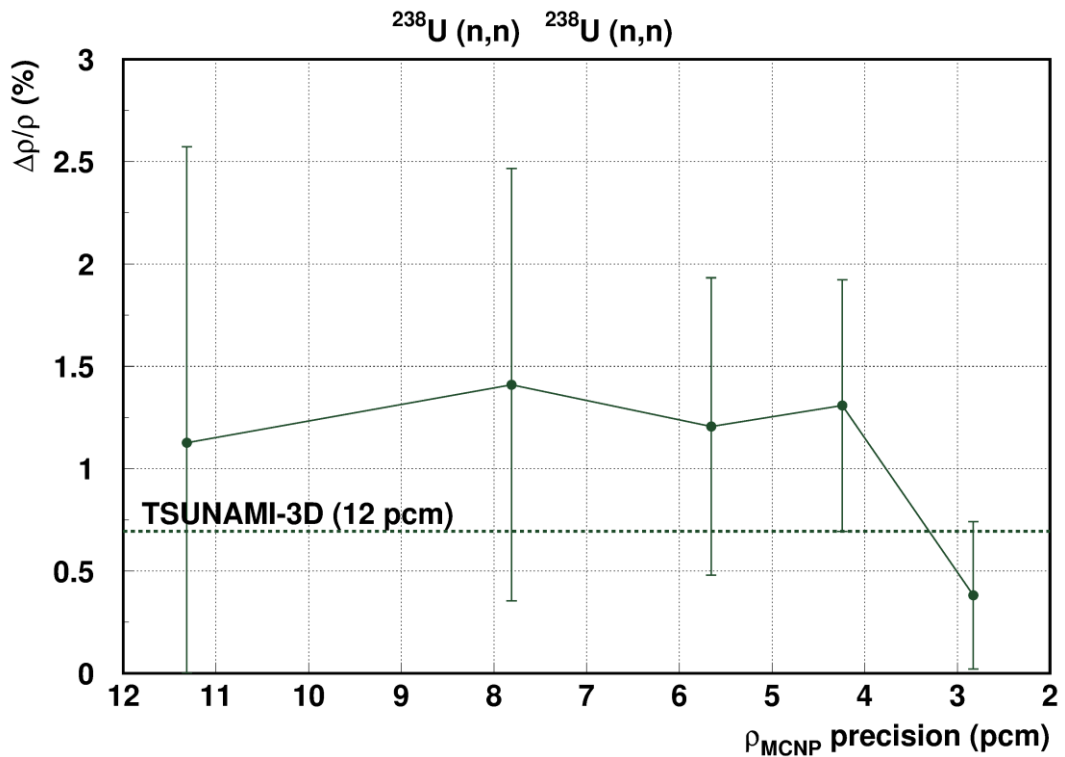
**Table 4. Major contributors to the uncertainty in the sodium void scenario of ESRF calculated with MCNP+SUMMON and TSUNAMI-3D.**

ESFR-RZ (sodium-void-scenario), JEFF-3.3 library, 33 groups						
		$\Delta\rho / \rho$ (%)				
Quantity		TSUNAMI-3D	TSUNAMI-3D + SUMMON		MCNP + SUMMON	
		+TSAR	Result	Ratio	Result	Ratio
$^{239}\text{Pu}(n,f)$	$^{239}\text{Pu}(n,f)$	5.086	5.085	1.0000	5.489	1.0792
		$\pm 5.32\text{E-}03$	$\pm 1.31\text{E-}02$	$\pm 0.0028$	$\pm 1.86\text{E-}01$	$\pm 0.0365$
$^{239}\text{Pu}(n,\gamma)$	$^{239}\text{Pu}(n,\gamma)$	2.406	2.406	0.9998	2.443	1.0154
		$\pm 6.02\text{E-}04$	$\pm 3.39\text{E-}03$	$\pm 0.0014$	$\pm 6.49\text{E-}02$	$\pm 0.0270$
$^{238}\text{U}(n,n')$	$^{238}\text{U}(n,n')$	1.911	1.871	0.9790	1.802	0.9431
		$\pm 1.19\text{E-}02$	$\pm 9.61\text{E-}02$	$\pm 0.0507$	$\pm 3.91\text{E-}01^*$	$\pm 0.2045$
$^{23}\text{Na}(n,n)$	$^{23}\text{Na}(n,n)$	1.843	1.840	0.9985	1.535	0.8330
		$\pm 9.12\text{E-}03$	$\pm 7.33\text{E-}02$	$\pm 0.0401$	$\pm 2.54\text{E-}01^*$	$\pm 0.1381$
$^{239}\text{Pu}(n,f)$	$^{239}\text{Pu}(n,\gamma)$	-1.781	-1.781	0.9998	-1.857	1.0428
		$\pm 5.31\text{E-}04$	$\pm 2.16\text{E-}03$	$\pm 0.0012$	$\pm 4.61\text{E-}02$	$\pm 0.0259$
$^{238}\text{U}(n,\gamma)$	$^{238}\text{U}(n,\gamma)$	1.721	1.717	0.9979	1.762	1.0239
		$\pm 4.13\text{E-}04$	$\pm 2.53\text{E-}03$	$\pm 0.0015$	$\pm 5.35\text{E-}02$	$\pm 0.0311$
$^{238}\text{U}(n,n')$	$^{238}\text{U}(n,\gamma)$	-1.623	-1.589	0.9793	-1.886	1.1622
		$\pm 6.78\text{E-}03$	$\pm 4.82\text{E-}03$	$\pm 0.0051$	$\pm 1.22\text{E-}01$	$\pm 0.0755$
$^{238}\text{U}(n,n)$	$^{238}\text{U}(n,n')$	-1.547	-1.519	0.9822	-1.050	0.6791
		$\pm 1.37\text{E-}02$	$\pm 7.61\text{E-}02$	$\pm 0.0499$	$\pm 2.24\text{E-}01^*$	$\pm 0.1446$
$^{241}\text{Pu}(n,f)$	$^{241}\text{Pu}(n,f)$	1.369	1.367	0.9987	1.457	1.0643
		$\pm 1.74\text{E-}03$	$\pm 1.18\text{E-}02$	$\pm 0.0087$	$\pm 8.82\text{E-}02$	$\pm 0.0644$
$^{23}\text{Na}(n,n')$	$^{23}\text{Na}(n,n')$	1.330	1.316	0.9893	1.309	0.9844
		$\pm 9.20\text{E-}04$	$\pm 8.52\text{E-}03$	$\pm 0.0064$	$\pm 3.33\text{E-}02^*$	$\pm 0.0251$
$^{23}\text{Na}(n,\gamma)$	$^{23}\text{Na}(n,\gamma)$	1.316	1.910	1.4516	1.984	1.5076
		$\pm 8.16\text{E-}05$	$\pm 1.38\text{E-}03$	$\pm 0.0011$	$\pm 2.83\text{E-}02$	$\pm 0.0215$
$^{56}\text{Fe}(n,n)$	$^{56}\text{Fe}(n,n)$	1.274	1.274	1.0000	1.181	0.9272
		$\pm 1.28\text{E-}02$	$\pm 1.15\text{E-}01$	$\pm 0.0911$	$\pm 2.65\text{E-}01^*$	$\pm 0.2082$
$^{238}\text{U}(n,n')$	$^{238}\text{U}(n,f)$	-1.044	-1.055	1.0106	-1.111	1.0639
		$\pm 2.82\text{E-}03$	$\pm 4.25\text{E-}02$	$\pm 0.0408$	$\pm 4.74\text{E-}01$	$\pm 0.4541$
$^{238}\text{U}(n,n)$	$^{238}\text{U}(n,\gamma)$	0.983	0.971	0.9882	0.970	0.9872
		$\pm 5.39\text{E-}03$	$\pm 2.15\text{E-}03$	$\pm 0.0058$	$\pm 4.04\text{E-}01$	$\pm 0.4111$
$^{240}\text{Pu}(n,f)$	$^{240}\text{Pu}(n,f)$	0.953	0.925	0.9708	0.948	0.9948
		$\pm 9.54\text{E-}03$	$\pm 5.12\text{E-}02$	$\pm 0.0546$	$\pm 2.58\text{E-}01$	$\pm 0.2704$
$^{56}\text{Fe}(n,\gamma)$	$^{56}\text{Fe}(n,\gamma)$	0.773	0.773	0.9994	0.736	0.9525
		$\pm 4.40\text{E-}04$	$\pm 4.49\text{E-}03$	$\pm 0.0058$	$\pm 8.20\text{E-}02$	$\pm 0.1061$
$^{238}\text{U}(n,n)$	$^{238}\text{U}(n,f)$	0.745	0.759	1.0187	0.970	1.3026
		$\pm 3.93\text{E-}03$	$\pm 2.99\text{E-}02$	$\pm 0.0405$	$\pm 4.04\text{E-}01$	$\pm 0.5424$
$^{240}\text{Pu}(n,f)$	$^{240}\text{Pu}(n,\gamma)$	0.697	0.687	0.9852	0.727	1.0425
		$\pm 2.81\text{E-}03$	$\pm 3.26\text{E-}03$	$\pm 0.0061$	$\pm 6.65\text{E-}02$	$\pm 0.0955$
$^{238}\text{U}(n,n)$	$^{238}\text{U}(n,n)$	0.694	0.685	0.9877	0.381	0.5488
		$\pm 4.05\text{E-}03$	$\pm 1.11\text{E-}01$	$\pm 0.1608$	$\pm 3.59\text{E-}01^*$	$\pm 0.5174$

\*Results calculated with 2 pcm in  $k_{\text{eff}}$  (~2.8 pcm in  $\rho_{\text{void}}$ ) instead 8 pcm (~11 pcm in  $\rho_{\text{void}}$ ).



(a) Na-23 elastic scattering.



(b) U238 elastic scattering.

Figure 4. Impact of the precision of the MCNP calculations on the contribution of  $^{23}\text{Na}$  and  $^{238}\text{U}$  scattering reactions to the uncertainty in the sodium void reactivity worth.

## 5. Summary and conclusions

The S/U analysis methodologies available in the TSUNAMI-3D, MCNP and MORET codes have been compared for the JEFF-3.3 library and two computed integral characteristics of a simplified RZ model of the ESFR reactor, namely  $k_{eff}$  and a partial sodium void reactivity worth.

In the case of  $k_{eff}$ , the differences in the ISCs between TSUNAMI-3D and MCNP (KSEN) are of the order of 1% for most cross sections considered. The difference with MORET is somewhat larger, but still less than 10%. Exceptions are scattering reactions (both elastic and inelastic), where the discrepancies can be very large. However, since the ISCs for these reactions are affected by large statistical errors, the results of the three codes are still in agreement. The discrepancy between codes in the uncertainty in  $k_{eff}$  has been found to be of the same order of magnitude as for the ISCs. In the case of MCNP and MORET, the uncertainties have been calculated with the SUMMON code.

As to the sodium void reactivity worth, only TSUNAMI-3D and MCNP have been intercompared, as MORET does not have the capability to perform S/U calculations of reactivity responses. The difference between TSUNAMI-3D and MCNP in the ISCs and the uncertainty contributions for individual reactions have found to be larger than in the case of  $k_{eff}$ , of the order of 10% for reactions other than scattering and (as in the case of  $k_{eff}$ ) much larger for scattering reactions. This can be explained by the fact that S/U calculations of sensitivity responses require the calculation of small differences between two relatively similar values. Furthermore, a significant dependence of the uncertainty contributions on the statistics of the MCNP calculation has been observed for the scattering reactions, which cannot be explained by statistical effects and requires further research.

## 6. Acknowledgements

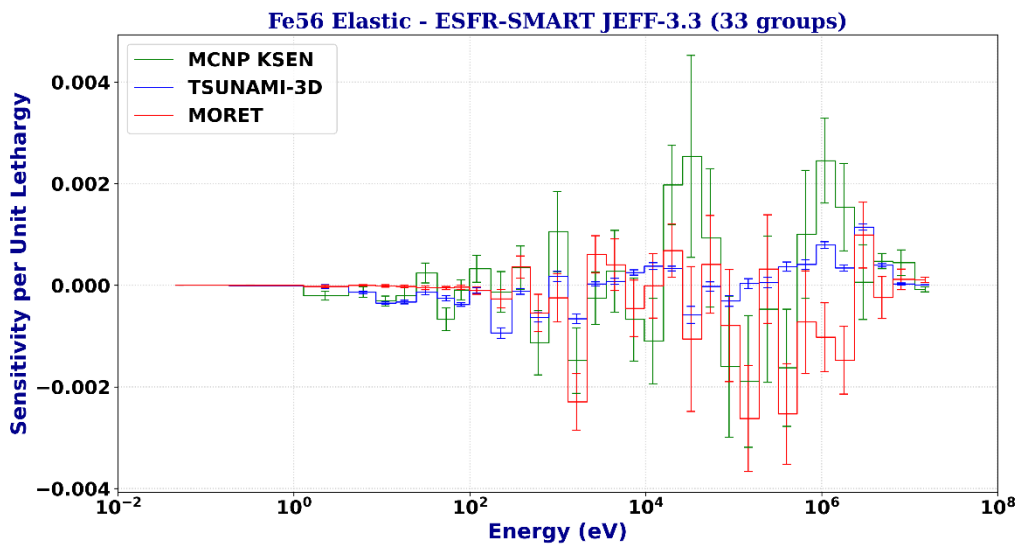
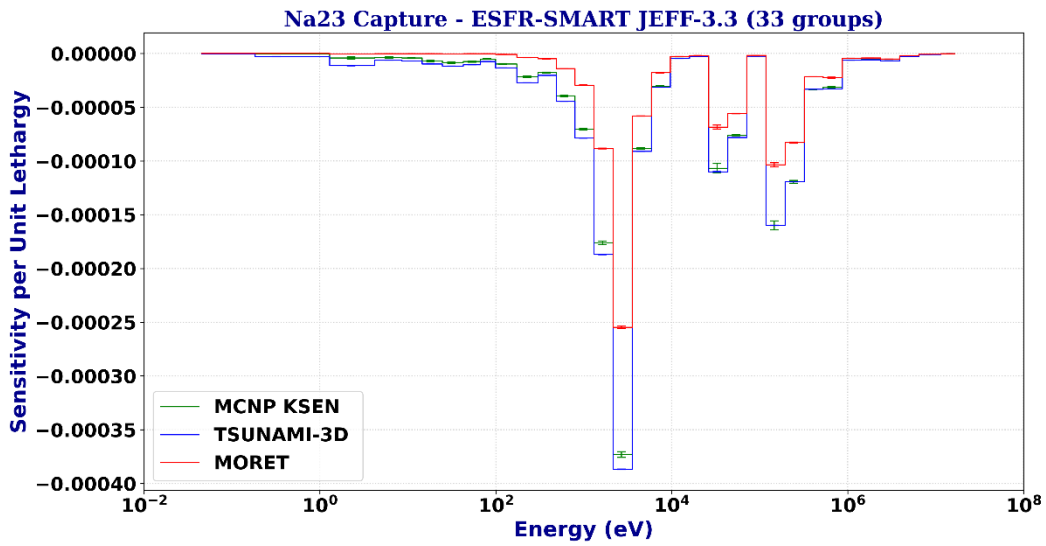
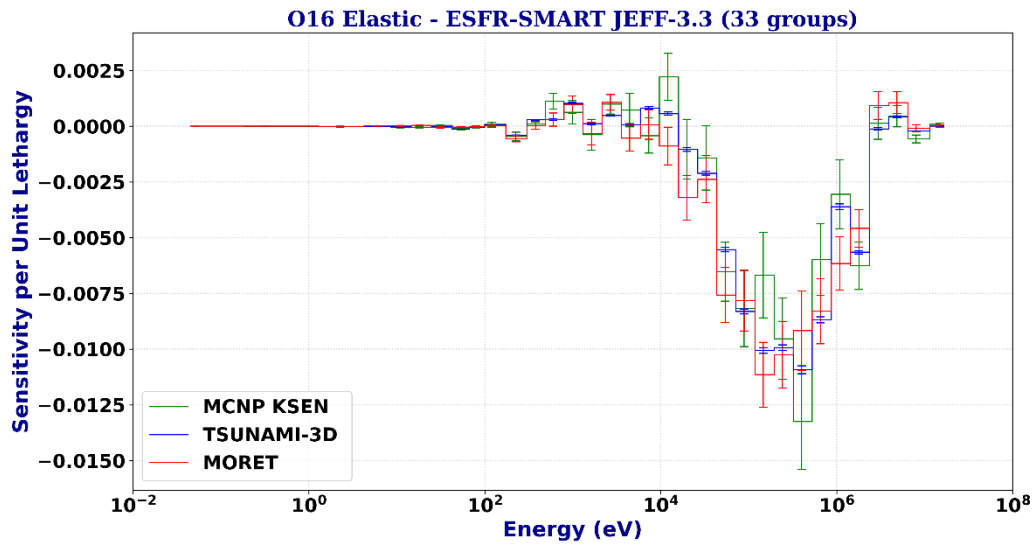
SCALE and MCNP have been obtained through NEA Computer Program Services and RSICC, respectively. The RZ ESFR model has been obtained through the NEA WPEC/SG46.

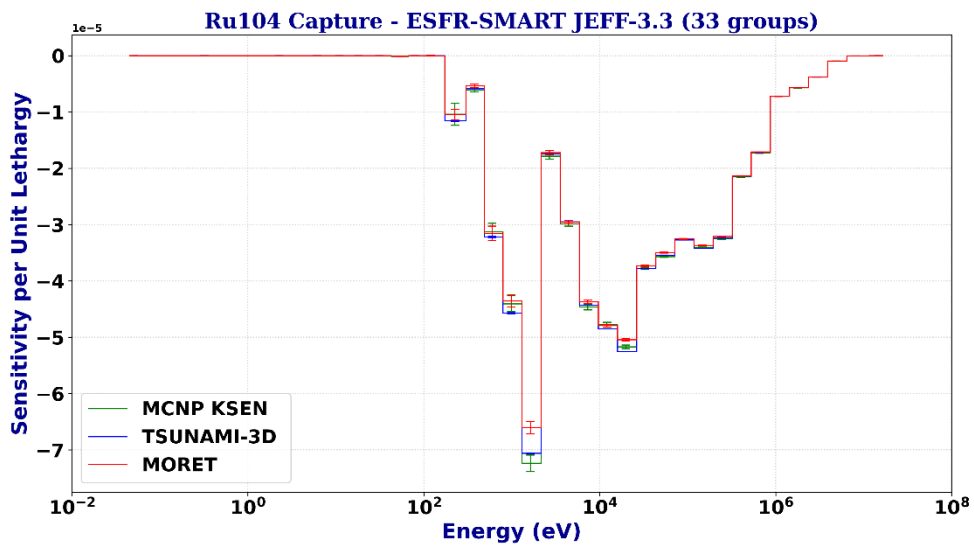
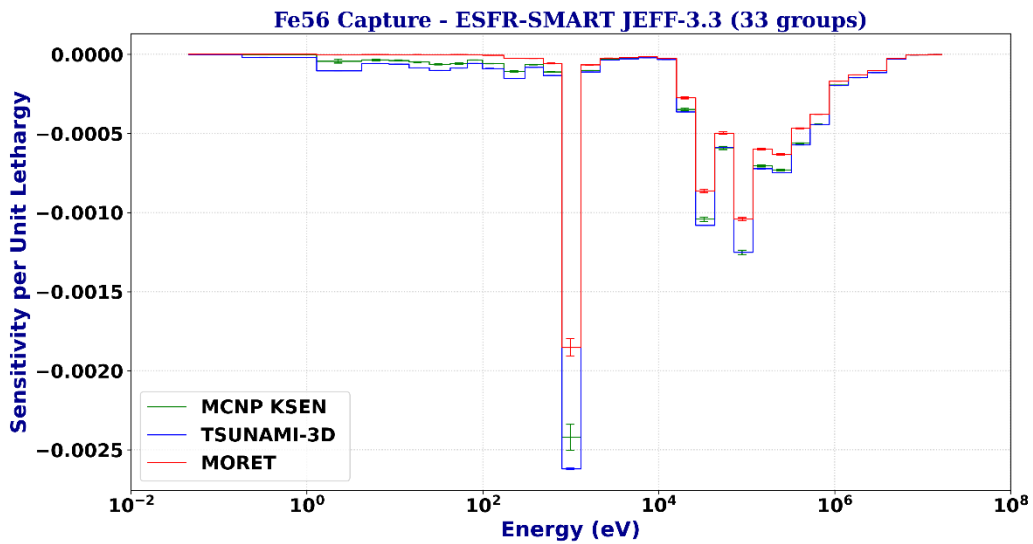
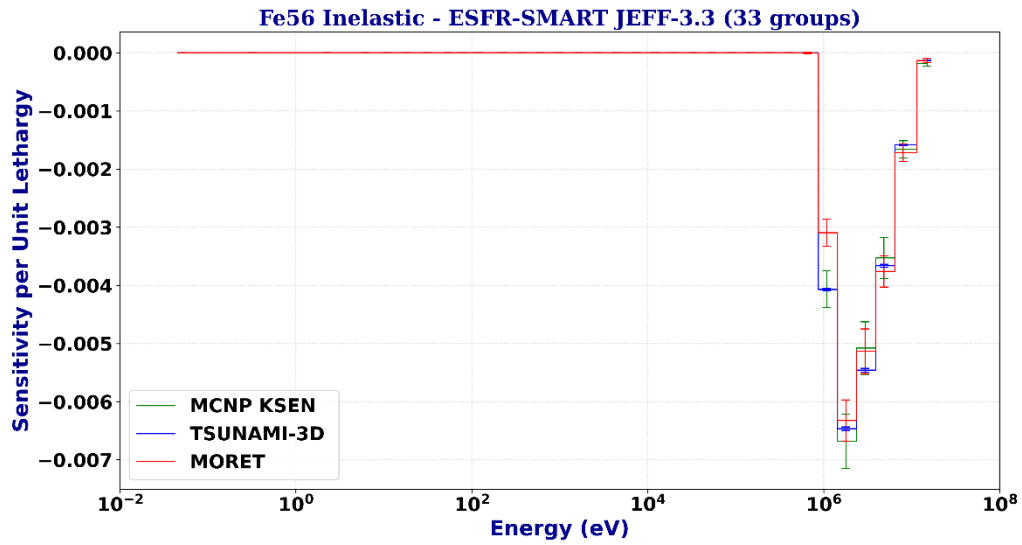
## 7. References

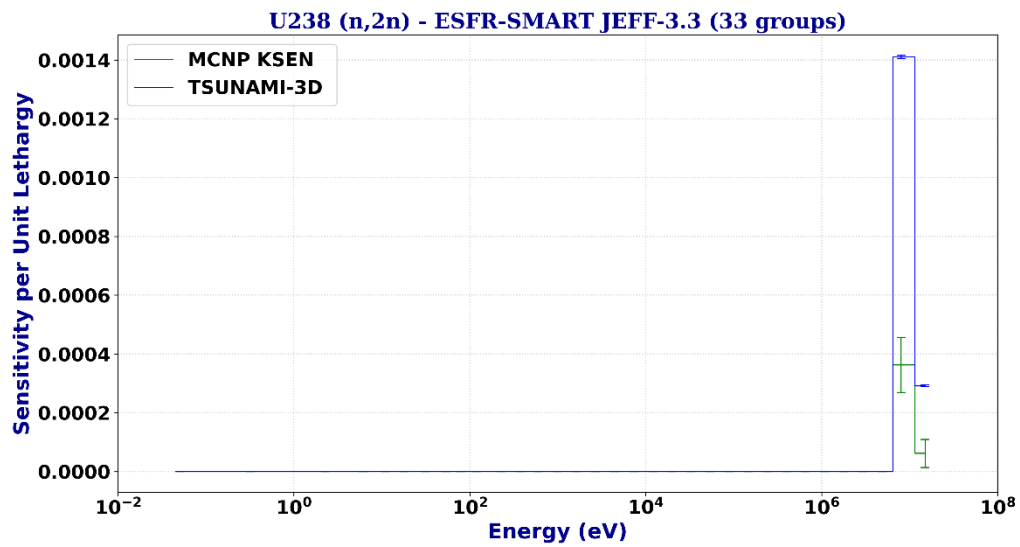
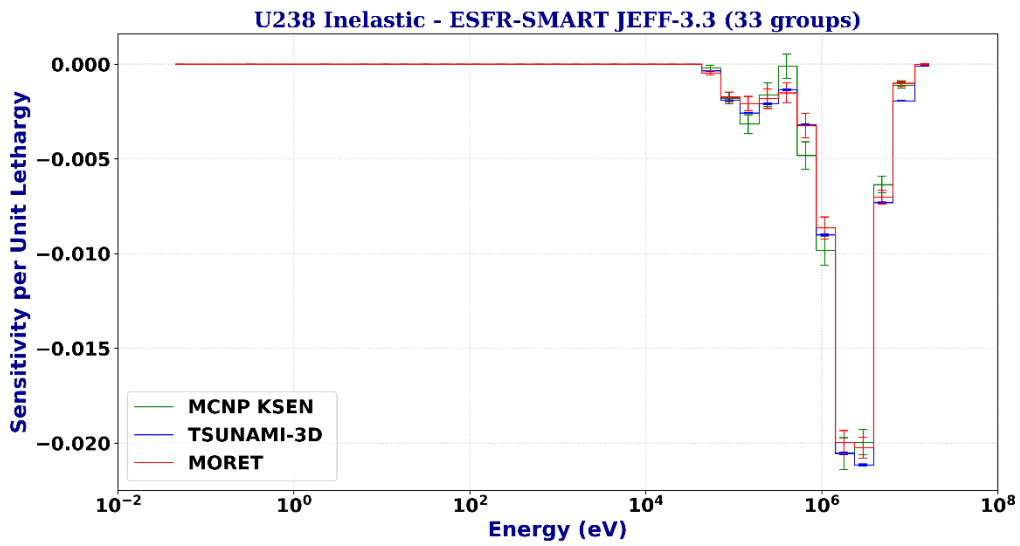
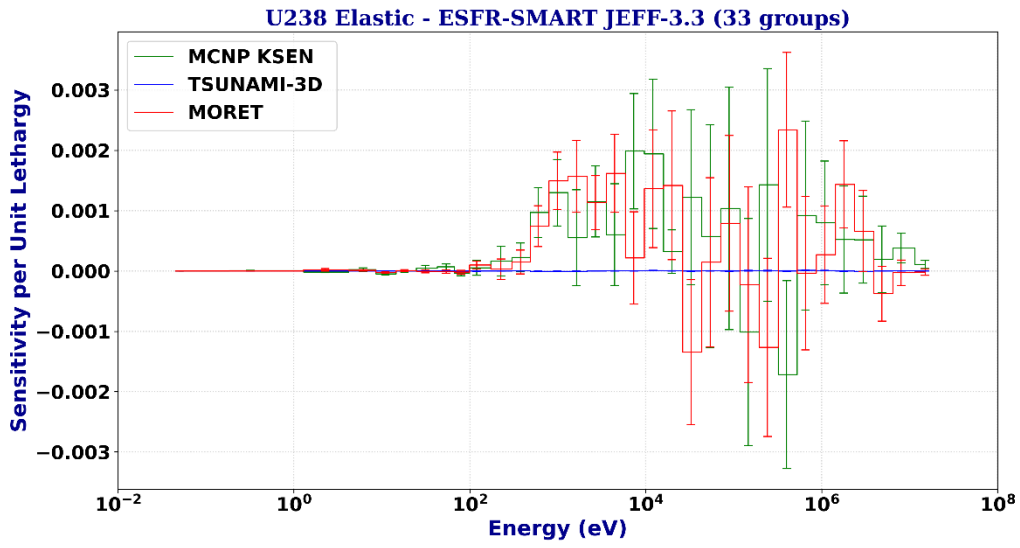
- [Blyskavka 2005] A. Blyskavka *et al.*, *Algorithm of Calculation of  $k_{eff}$  Sensitivities to Group Cross Sections Using Monte Carlo Method and Features of Its Implementation in the MMKKENO Code*. In M&C 2005, Avignon (France), 12-15 September 2005.
- [Cacuci 2003] D. G. Cacuci, *Sensitivity and Uncertainty Analysis Vol. I. Theory*. Chapman & Hall/CRC, 2003.
- [Davies 2020] U. Davies *et al.*, *Evaluation of the ESFR end of cycle state and detailed analysis of spatial distributions of reactivity coefficients*. In PHYSOR 2020, Cambridge (UK) 28 March – 2 April 2020 (also available in EPJ Web of Conferences 247 (2021) 02001).
- [Haeck 2015] W. Haeck *et al.*, *GAIA User's Manual - Version 1.0.0*, IRSN Report PSN-EXP/SNC/2015-165, Institut de Radioprotection et de Sûreté Nucléaire, France (2015).
- [Jiménez-Carrascosa 2020] A. Jiménez-Carrascosa *et al.*, *Joint UPM and CIEMAT contribution: Progress on ESFR, WPEC Subgroup 46 (SG46) WebEx meeting, 11 November 2020* (<https://www.oecd-nea.org/download/wpec/sg46/meetings/2020-11/>)
- [Jinaphanh 2016] A. Jinaphanh *et al.*, *Continuous-Energy Sensitivity Coefficients in the MORET Code*. Nuclear Science and Engineering 184 (2016) 53-68.
- [Jinaphanh 2017] A. Jinaphanh, *Implementation of the CLUTCH method in the MORET code*. In M&C 2017, Jeju (Korea) 16-20 April 2017.
- [Kiedrowski 2011a] B. C. Kiedrowski and F. B. Bown, *Comparison of the Monte Carlo Adjoint-Weighted and Differential Operator Perturbation Methods*. Progress in Nuclear Science and Technology 2 (2011) 836-841.

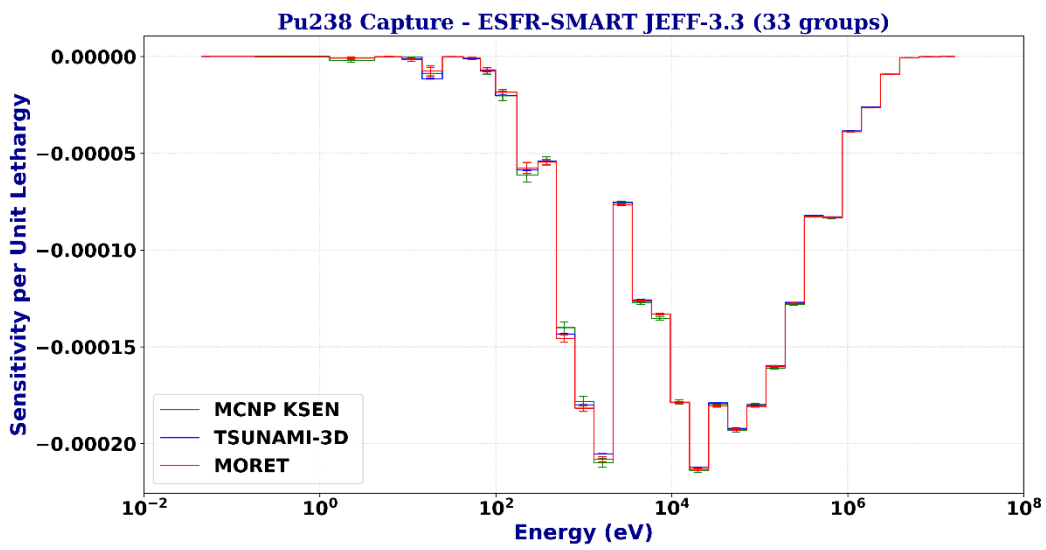
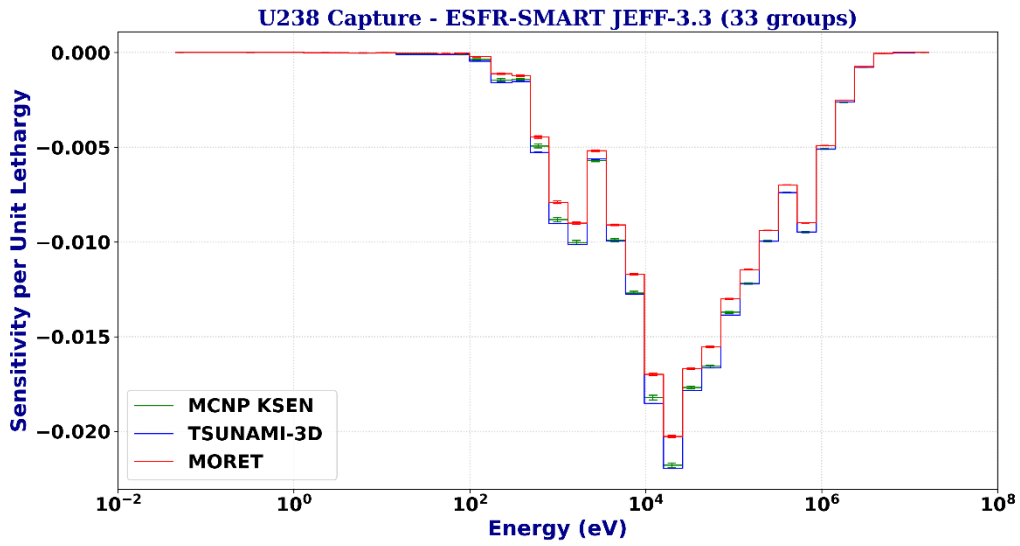
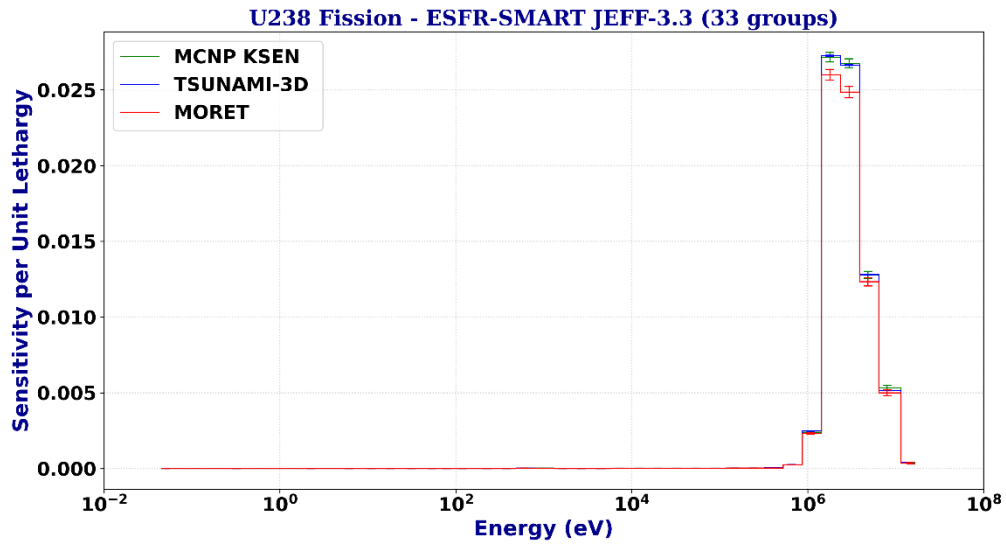
- [Kiedrowski 2011b] B. C. Kiedrowski and F. B. Brown, *Adjoint-Weighted Tallies for k-Eigenvalue Calculations with Continuous-Energy Monte Carlo*. Nuclear Science and Engineering 168 (2011) 226-241.
- [Kiedrowski 2012] B. C. Kiedrowski and F. B. Brown, *Continuous-Energy Sensitivity Coefficient Capability in MCNP6*. Los Alamos National Laboratory report LA-UR-12-21010 (2012).
- [MacFarlane 2016] R. E. MacFarlane *et al.*, *The NJOY Nuclear Data Processing System, Version 2016*. Los Alamos National Laboratory report LA-UR-17-20093 (2016).
- [Mikityuk 2017] K. Mikityuk *et al.*, *ESFR-SMART: New Horizon-2020 Project on SFR Safety*. AQ6 474 Proc. IAEA FR2017, Ekaterinburg (Russian Federation).
- [Nauchi 2010] Y. Nauchi and T. Kameyama, *Development of Calculation Technique for Iterated Fission Probability and Reactor Kinetic Parameters Using Continuous-Energy Monte Carlo Method*. Journal of Nuclear Science and Technology 47 (2010) 977-990.
- [Perfetti 2017] C. M. Perfetti *et al.*, *SCALE Continuous-Energy Eigenvalue Sensitivity Coefficient Calculations*. Nuclear Science and Engineering 182 (2016) 332-353.
- [Rearden 2011] B. T. Rearden *et al.*, *Sensitivity and Uncertainty Analysis Capabilities and Data in SCALE*. Nuclear Technology 174 (2011) 236-288.
- [Rearden 2018] B. T. Rearden and M. A. Jessee (Eds.), *SCALE Code System*. Oak Ridge National Laboratory report ORNL/TM-2005/39 Version 6.2.3 (2018).
- [Romojaro 2017] P. Romojaro *et al.*, *SUMMON: A Sensitivity And Uncertainty Methodology For MONte Carlo Codes*. In M&C 2017 Conference, Jeju (Korea) 16-20 April 2017.
- [Romojaro 2019] P. Romojaro *et al.*, *Sensitivity methods for effective delayed neutron fraction and neutron generation time with SUMMON*. Annals of Nuclear Energy 126 (2019) 410–418.
- [Romojaro 2021] P. Romojaro *et al.*, *On the importance of target accuracy assessments and data assimilation for the co-development of nuclear data and fast reactors: MYRRHA and ESFR*. Annals of Nuclear Energy 161 (2021) 1-13.
- [Werner 2017] C. J. Werner (Ed.), *MCNP User's Manual. Code Version 6.2*. Los Alamos National Laboratory Report LA-UR-17-29981 (2017).
- [Wiarda 2016] D. Wiarda *et al.*, *AMPX-6: A Modular Code System for Processing ENDF/B*. Oak Ridge National Laboratory report ORNL/TM-2016/43 (2016).

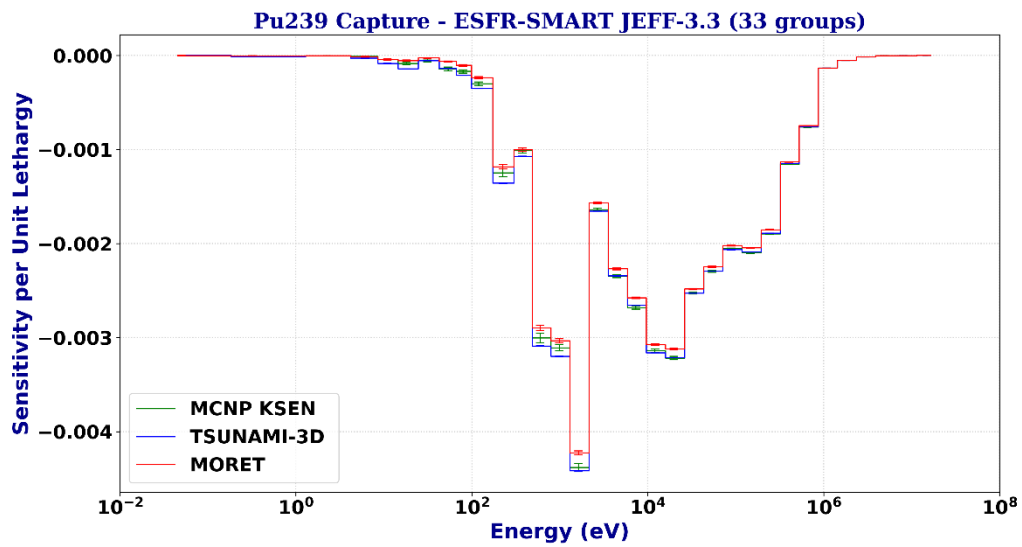
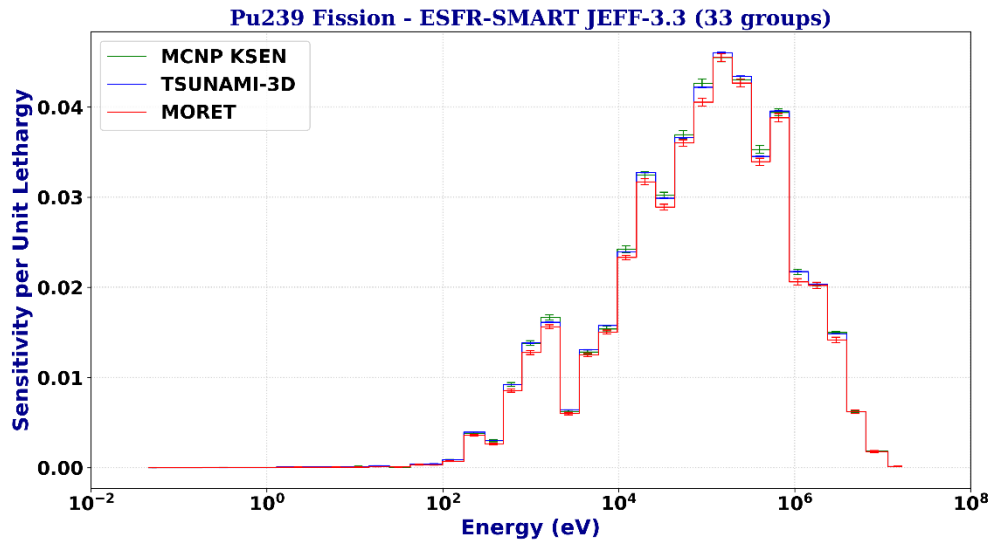
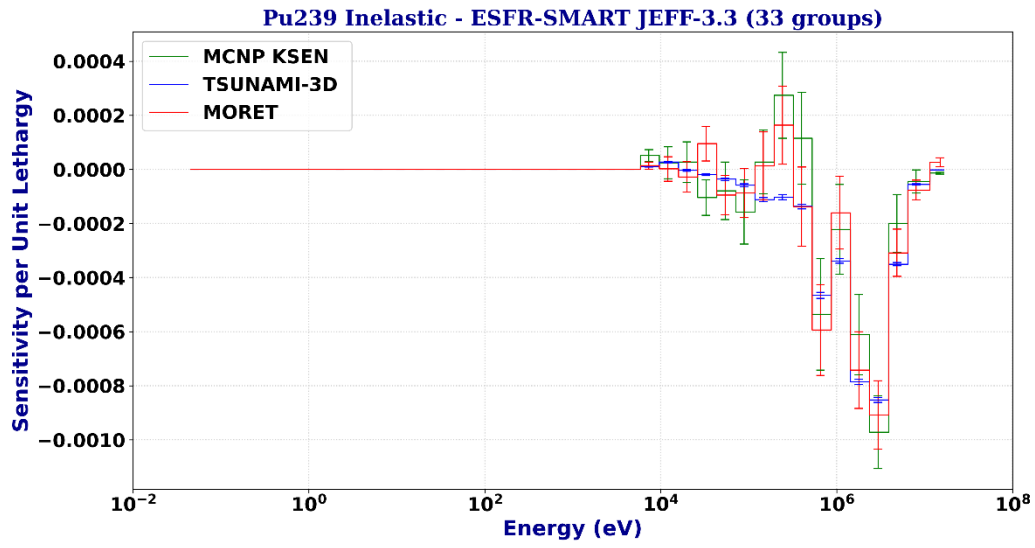
Annex 1. Sensitivity profiles for  $k_{eff}$

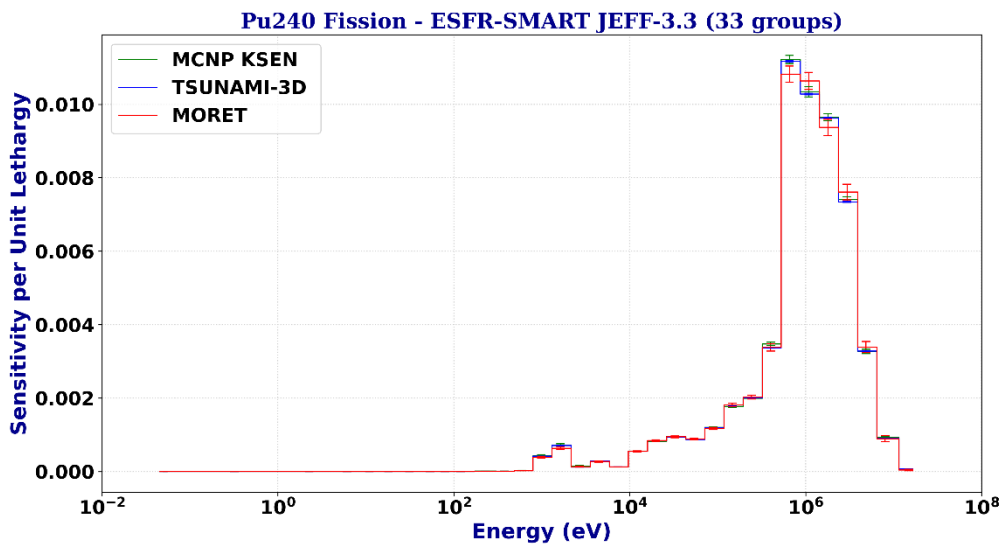
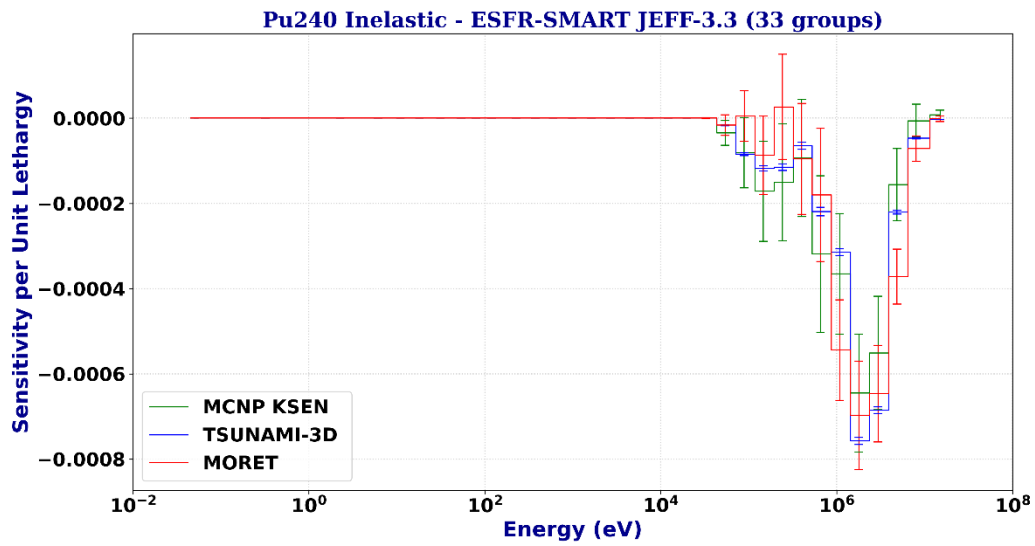
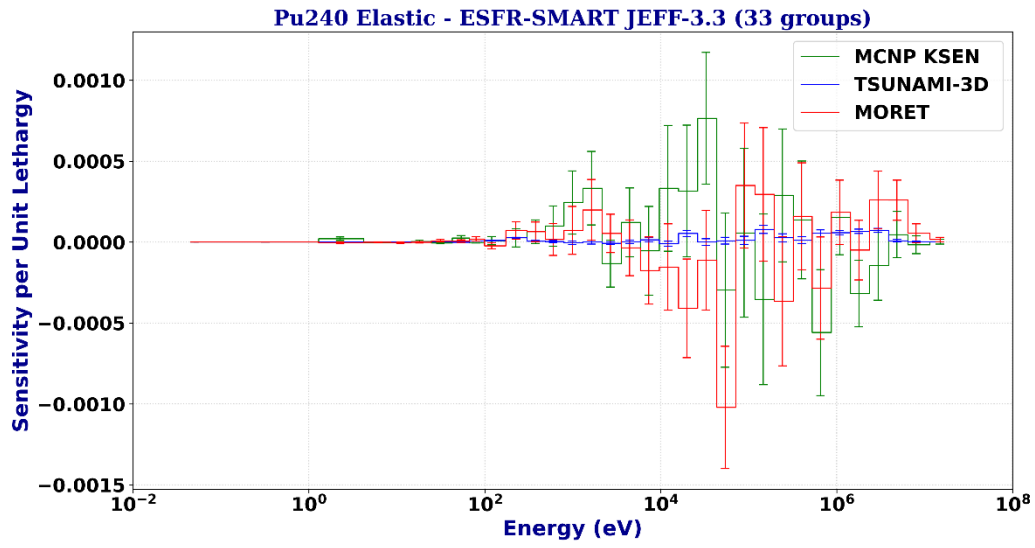


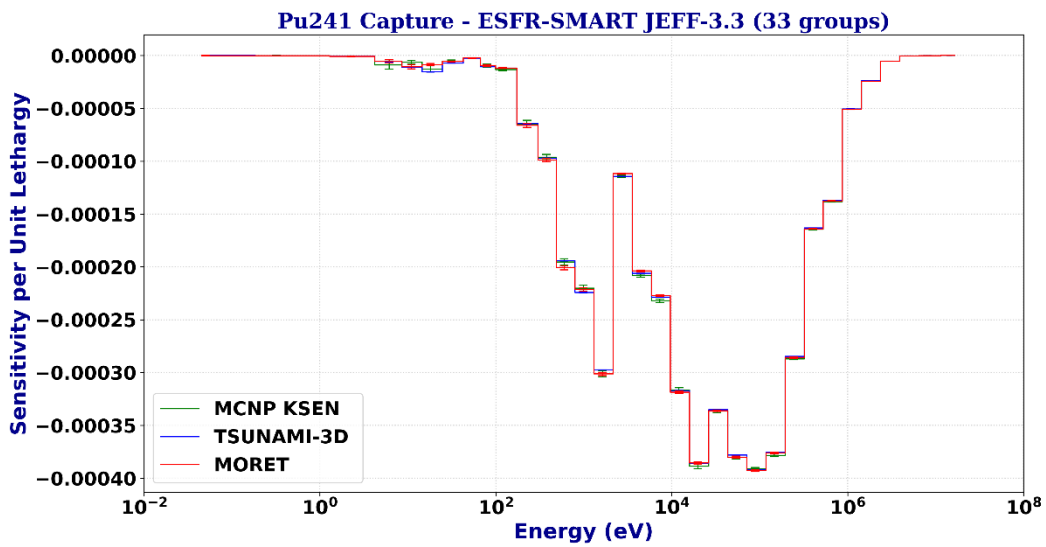
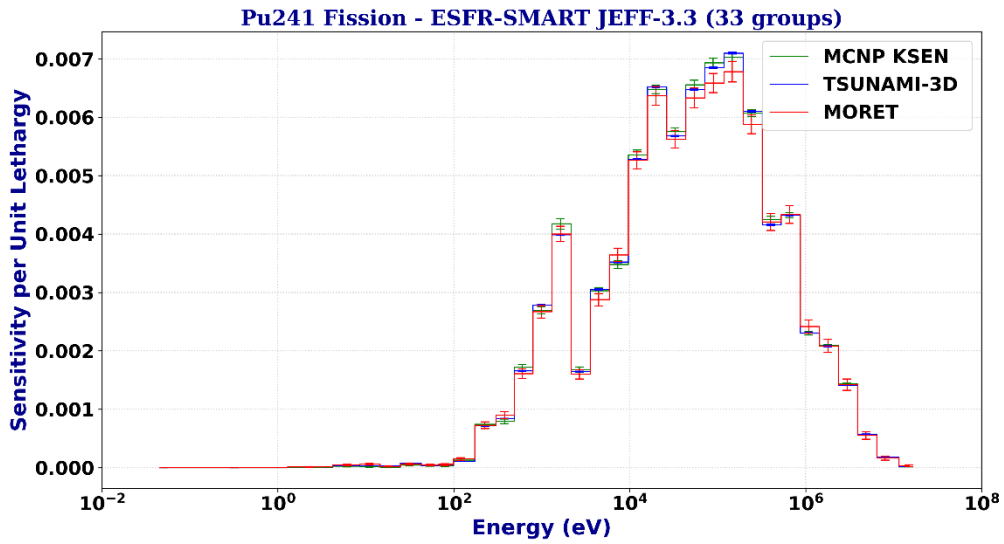
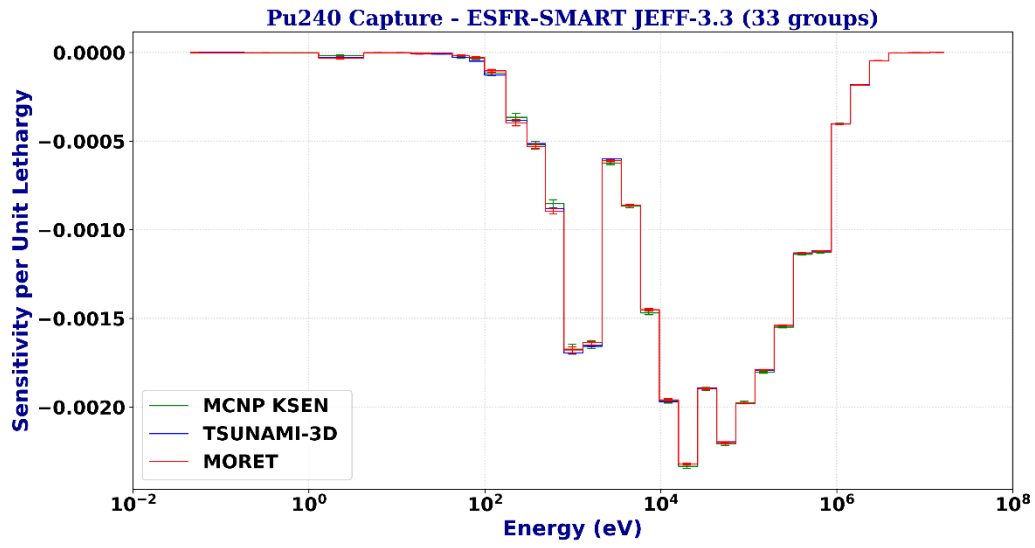




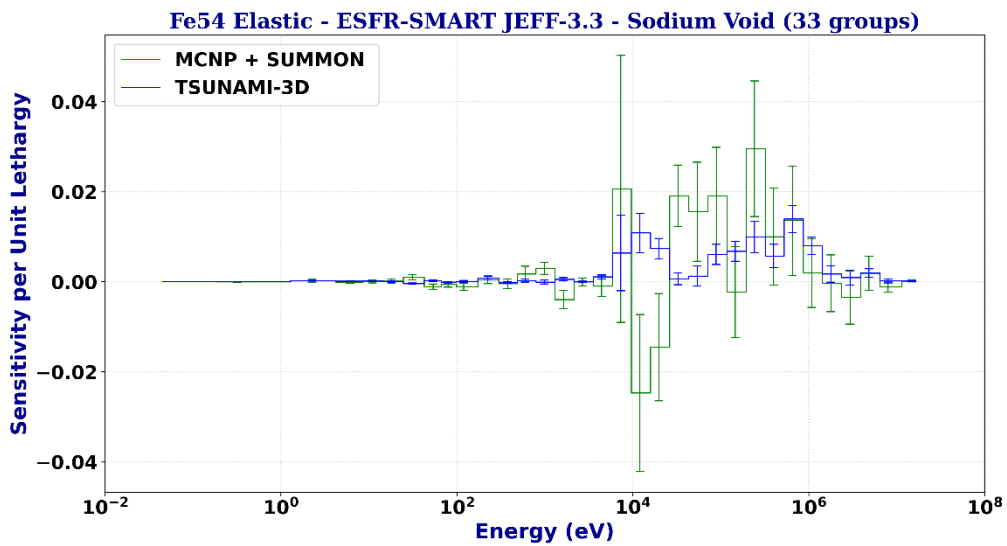
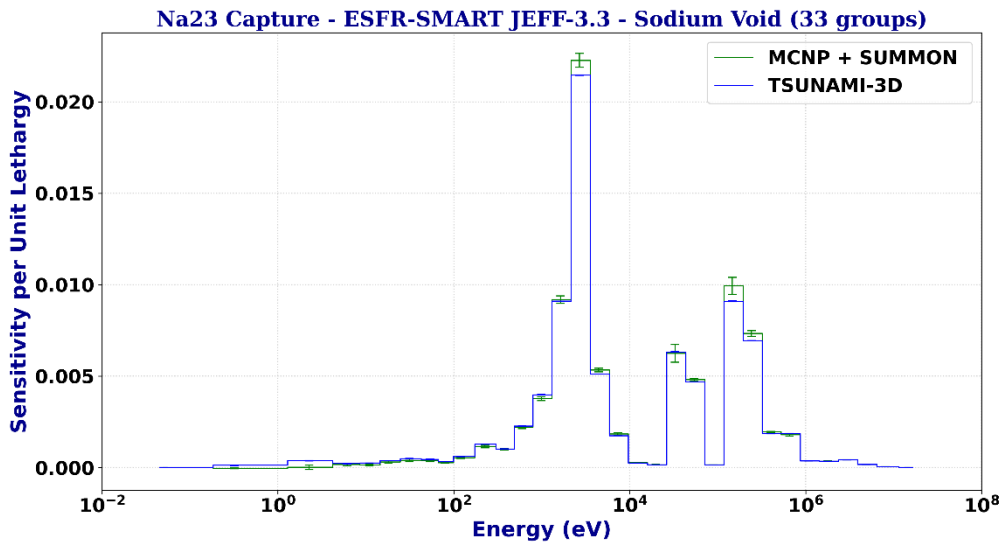
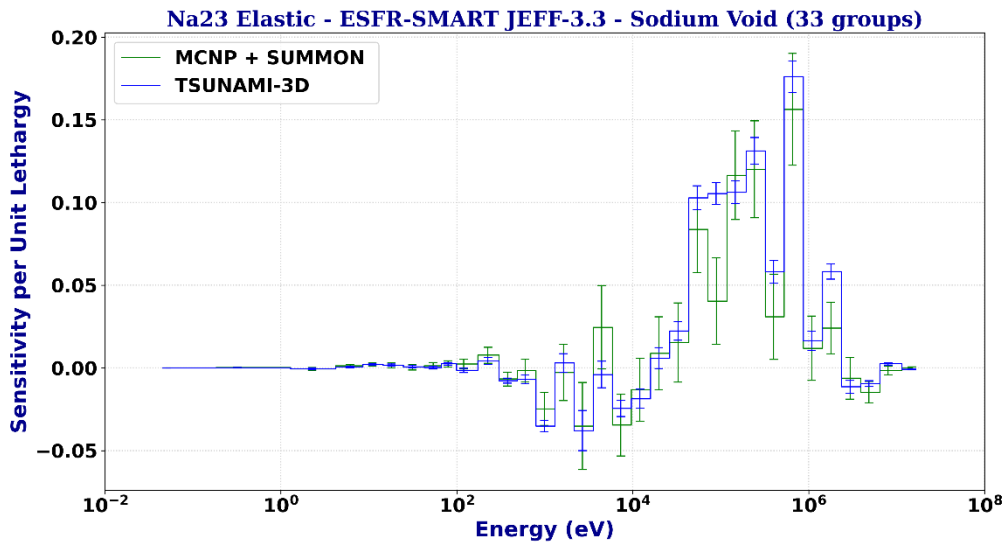


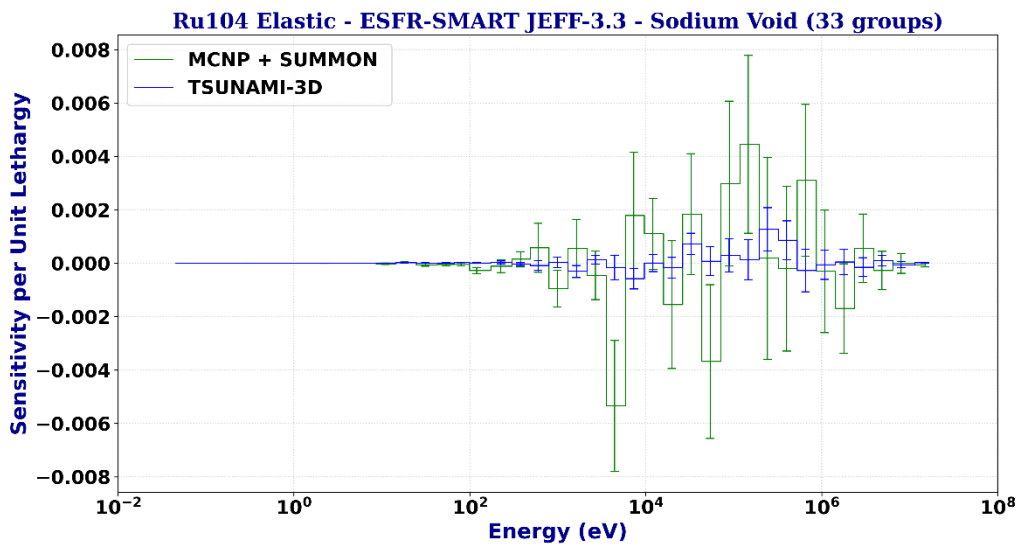
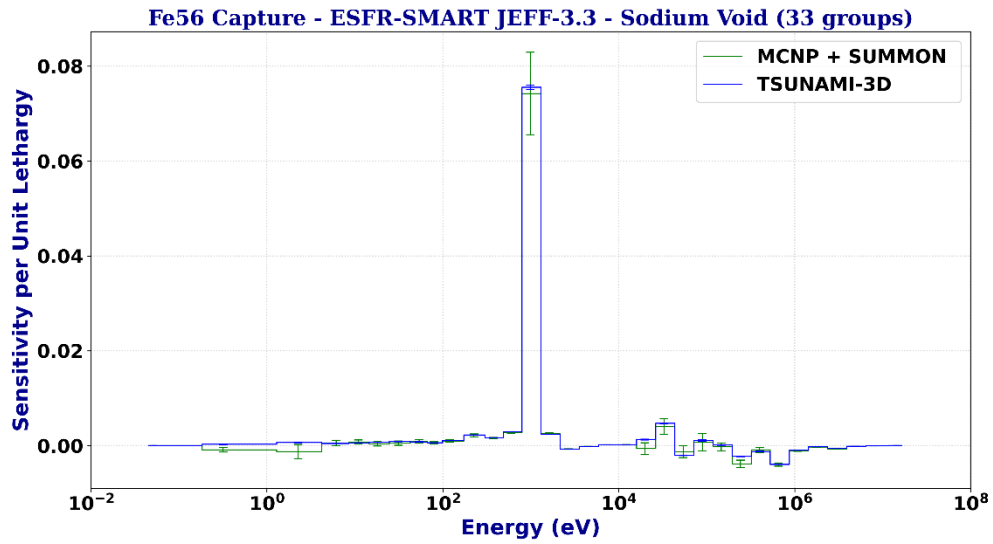
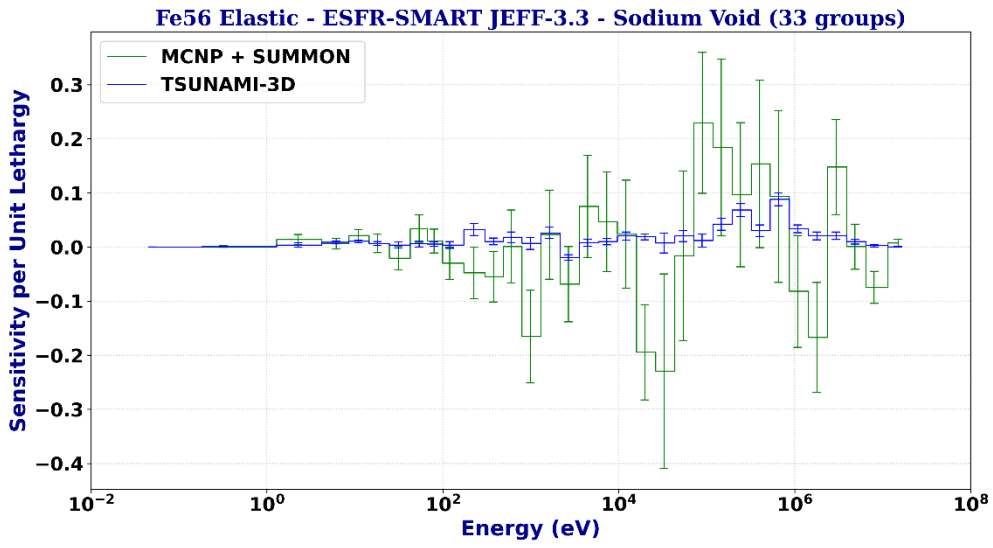


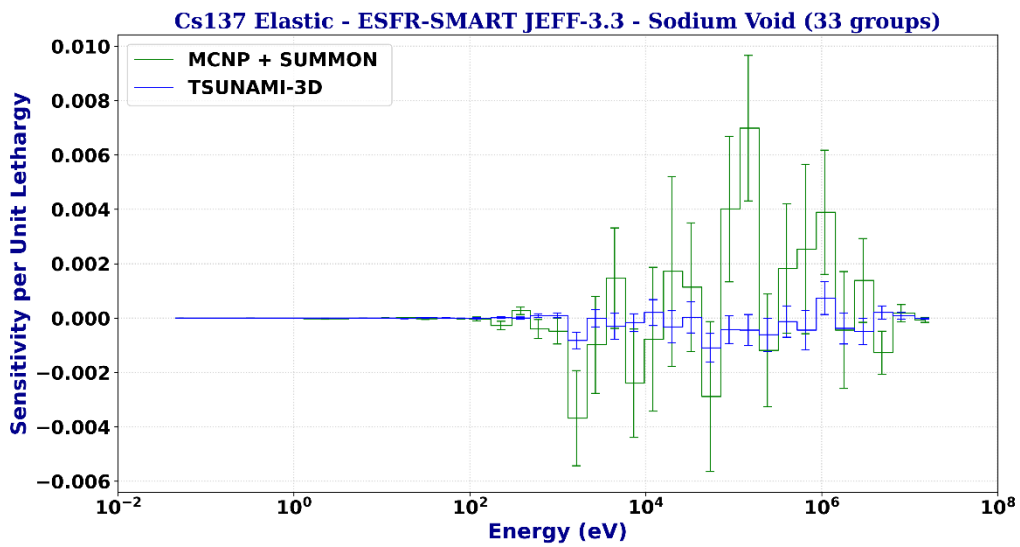
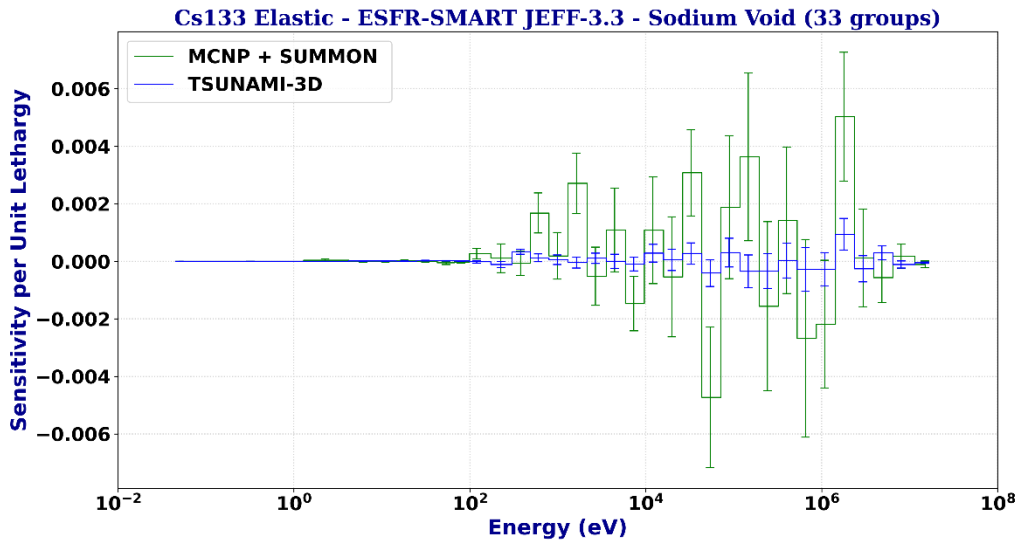
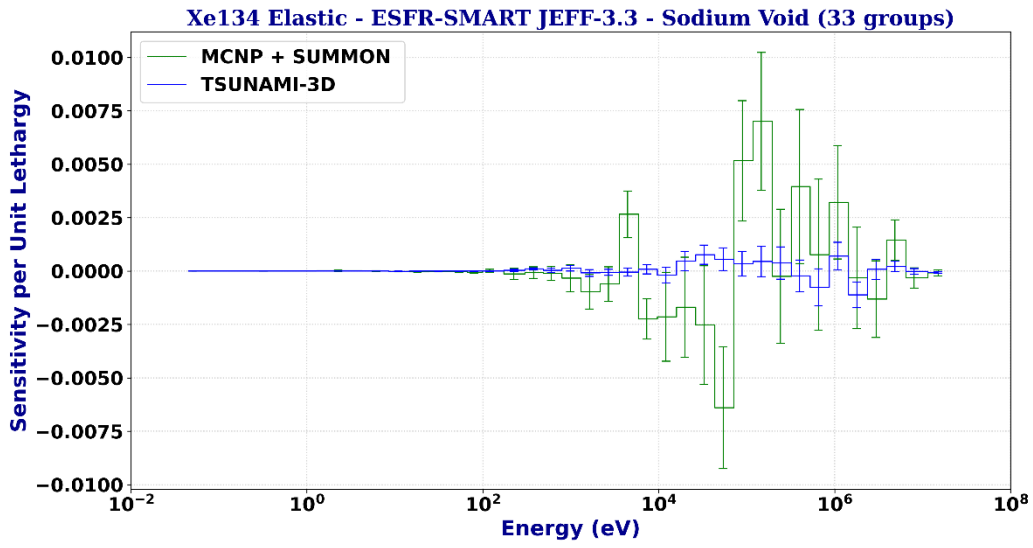


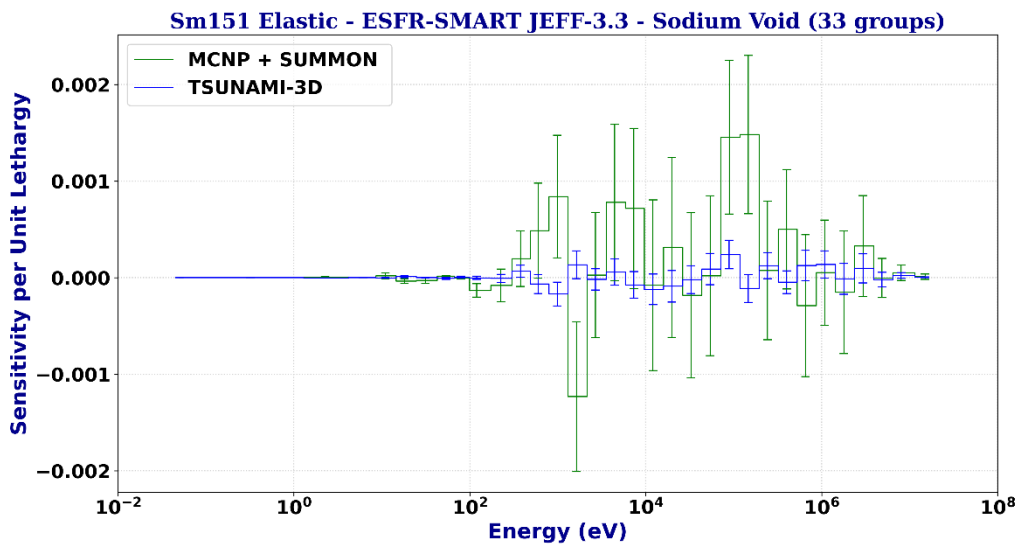
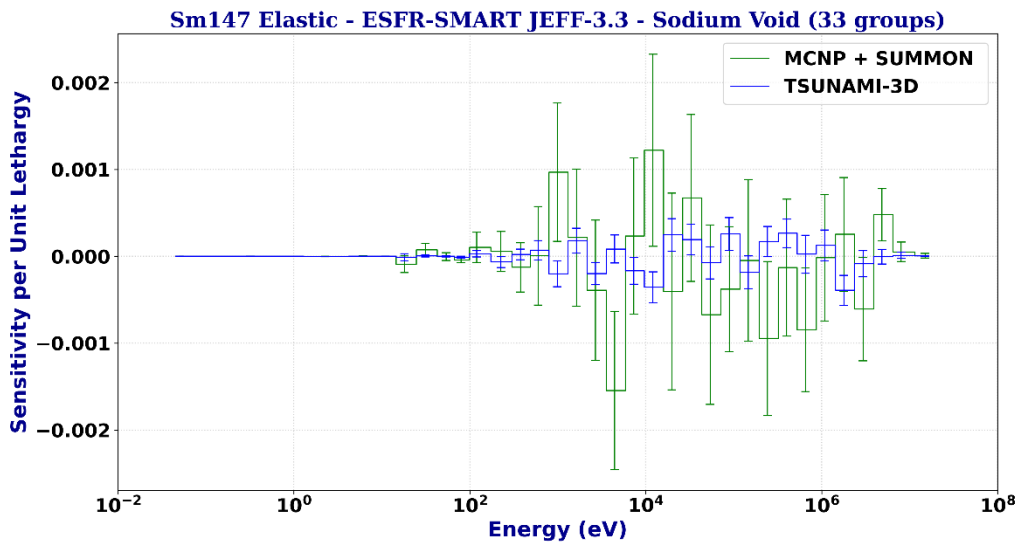
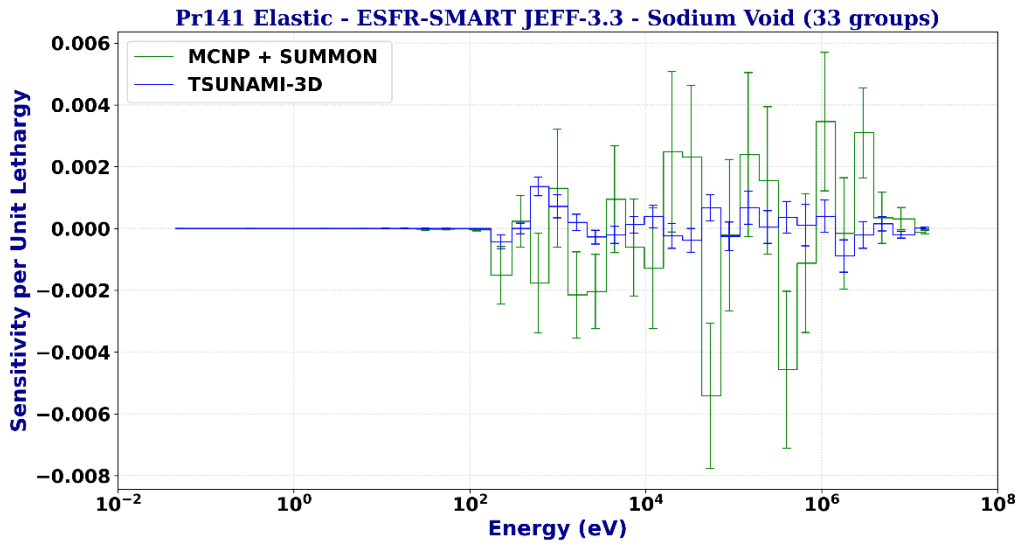


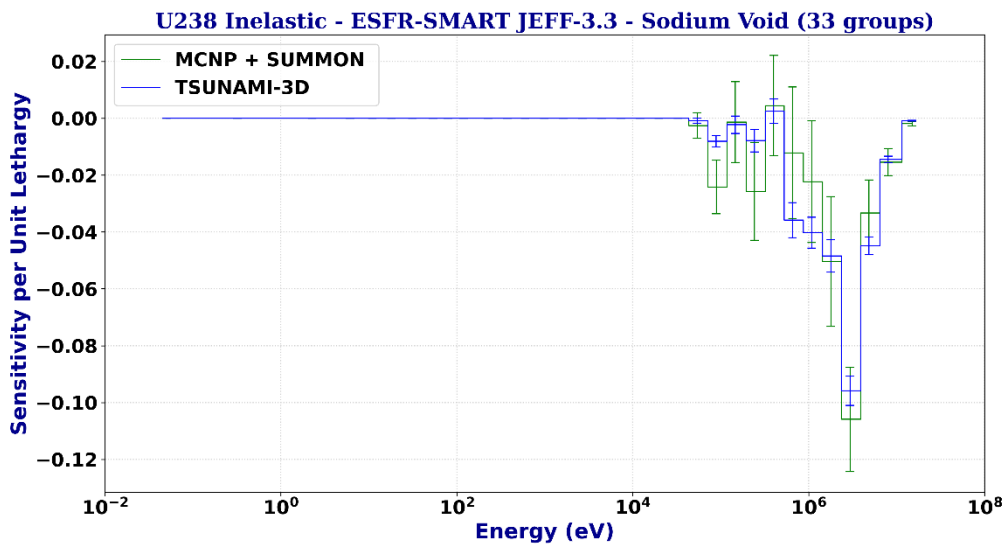
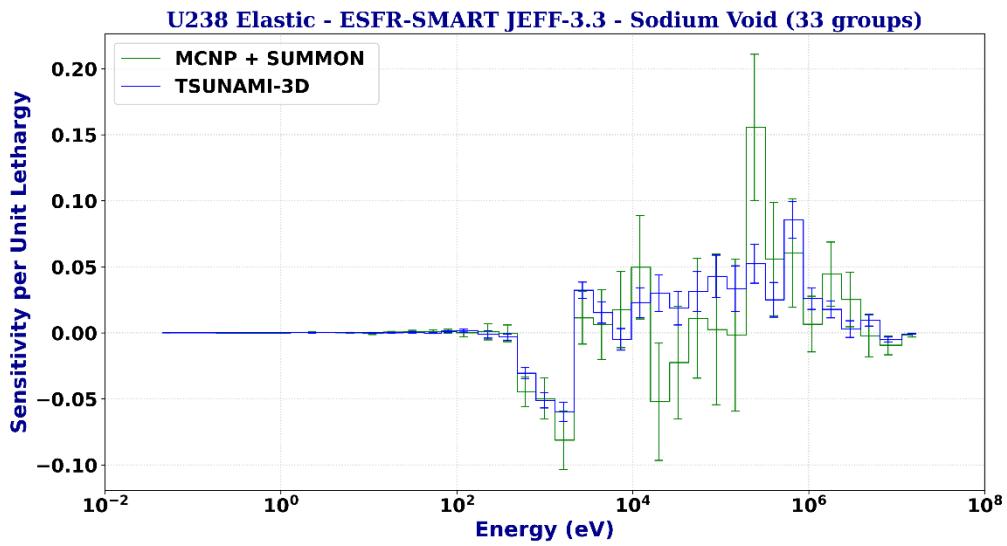
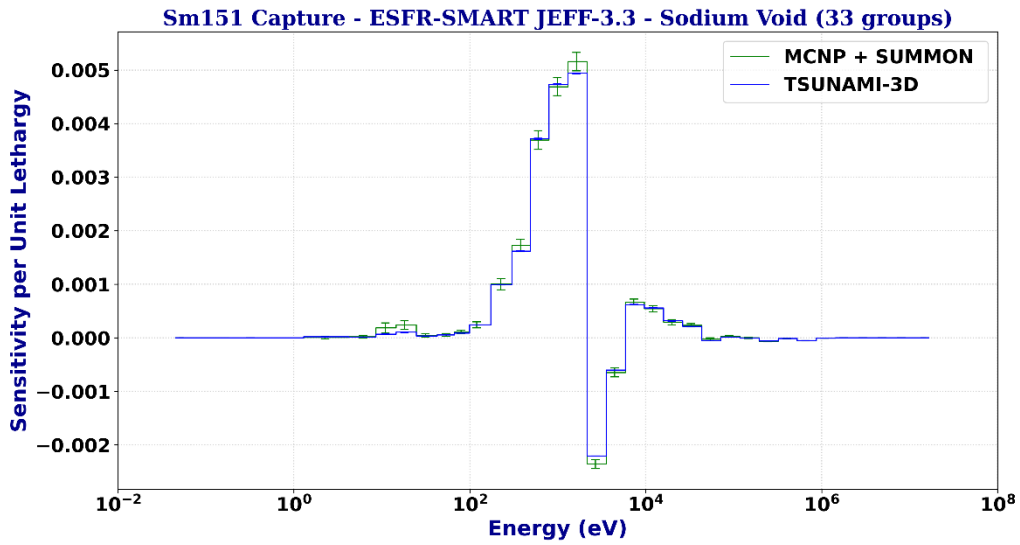
Annex 2. Sensitivity profiles for  $\rho_{Void}$

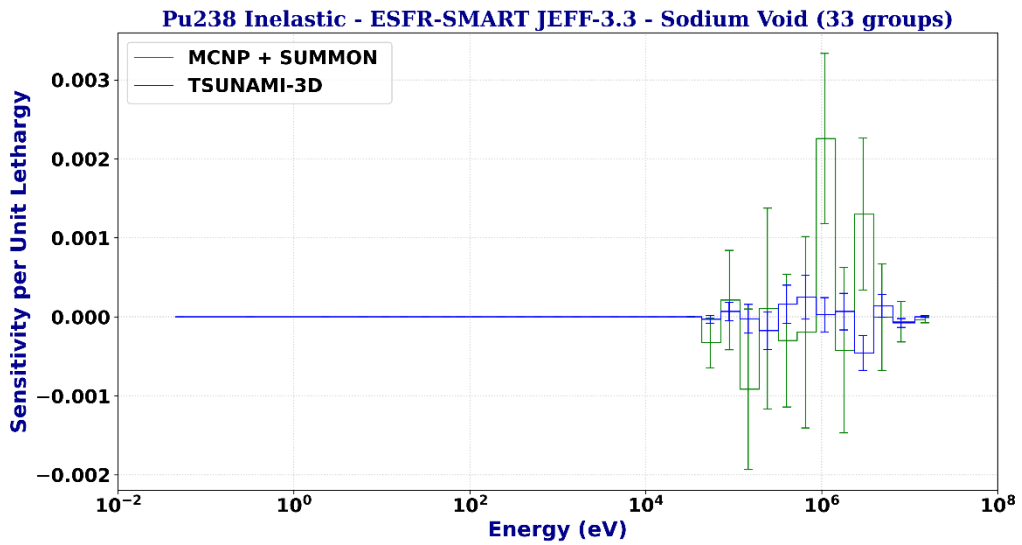
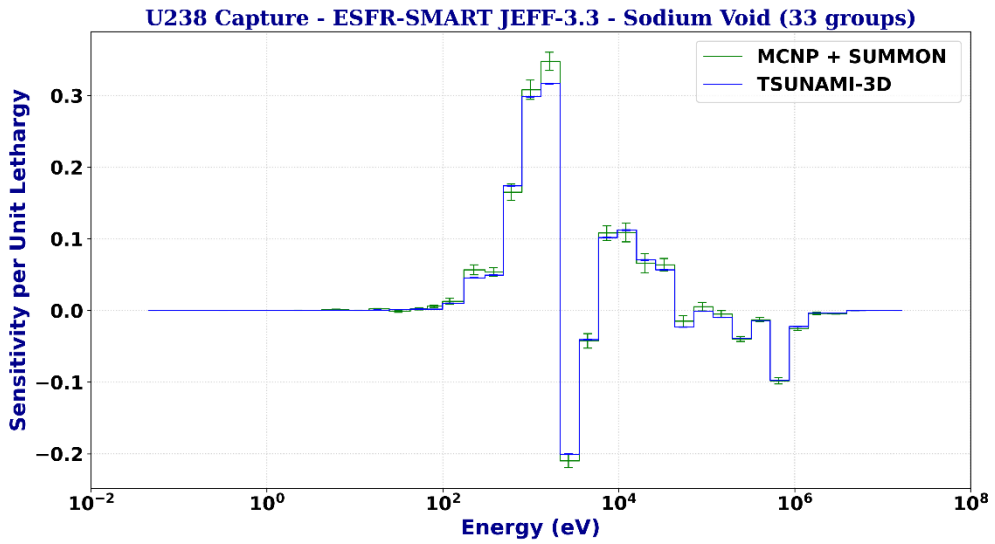
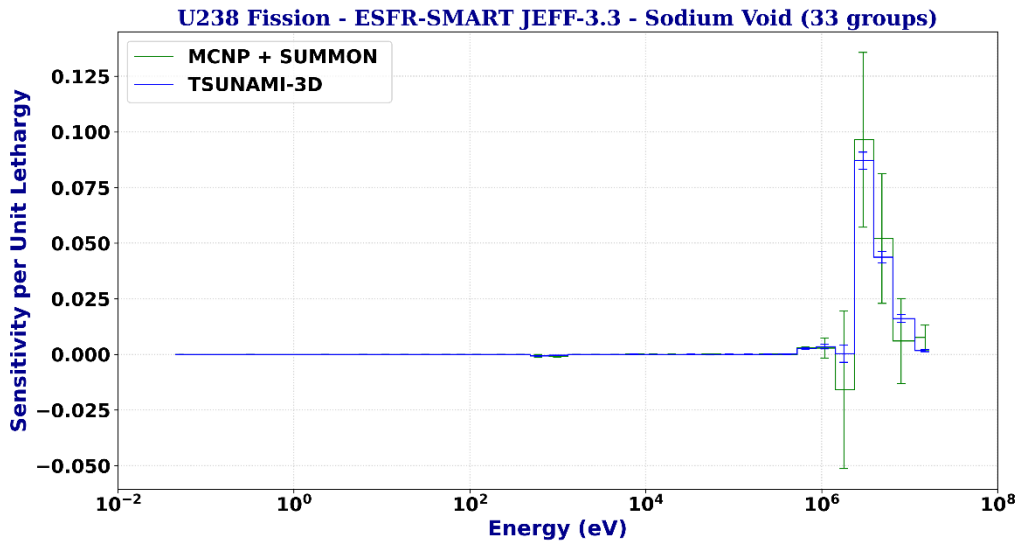


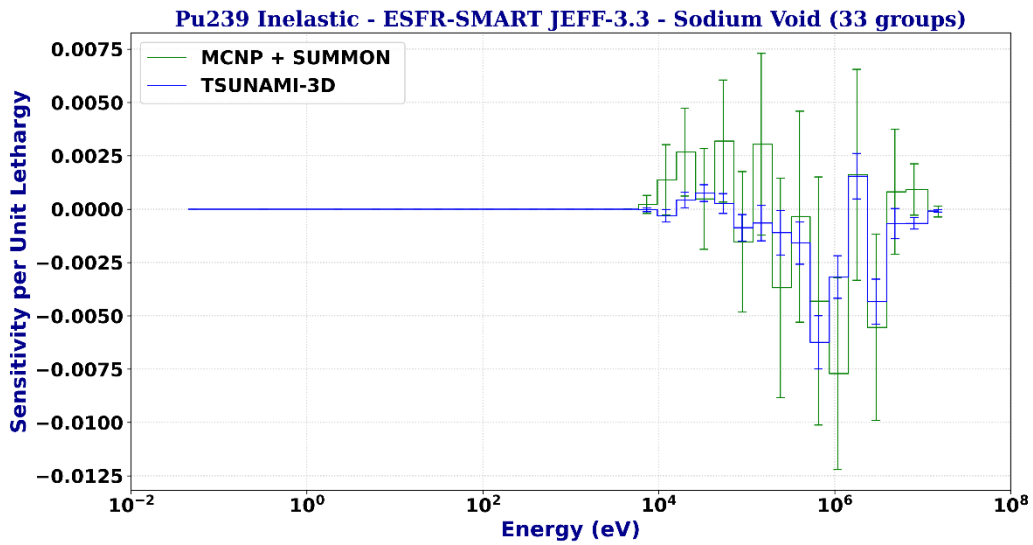
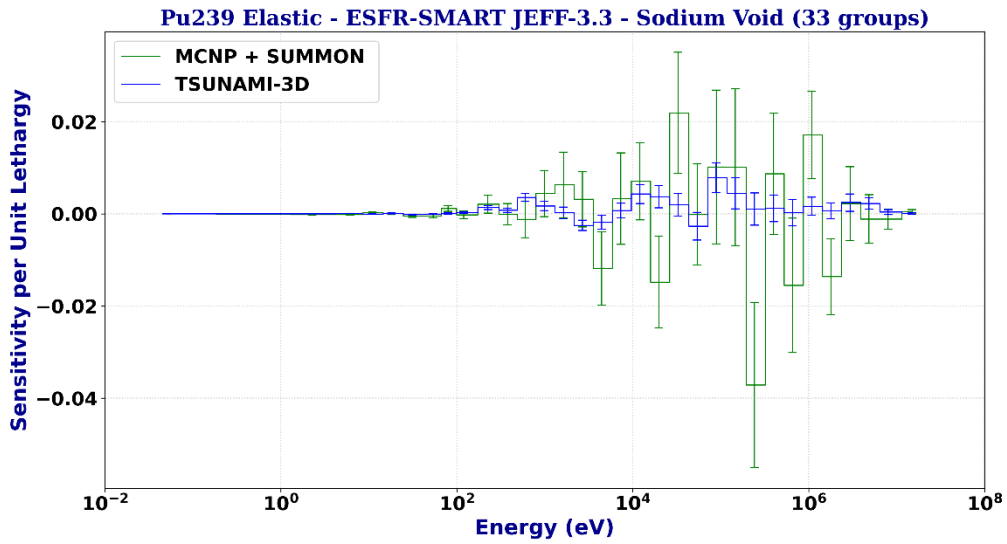
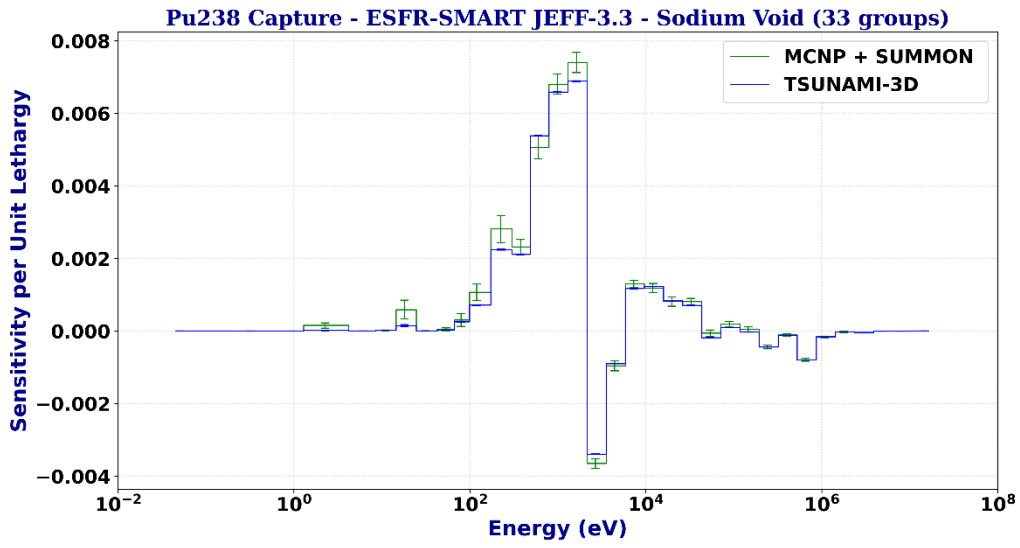


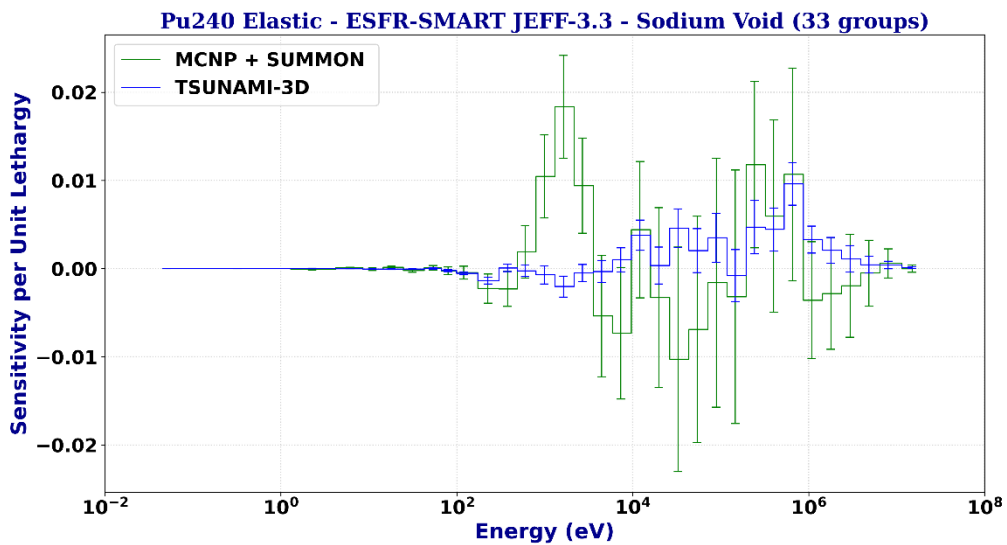
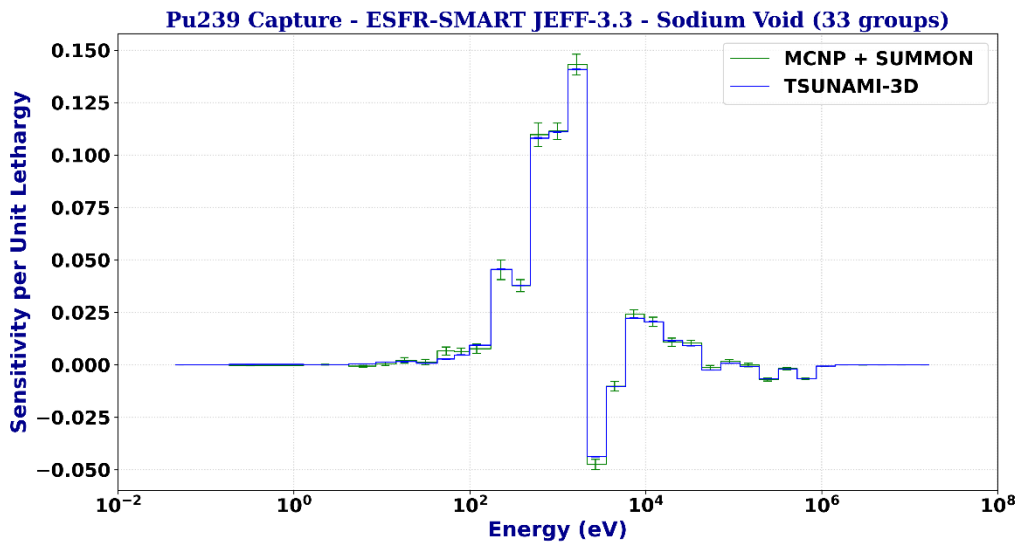
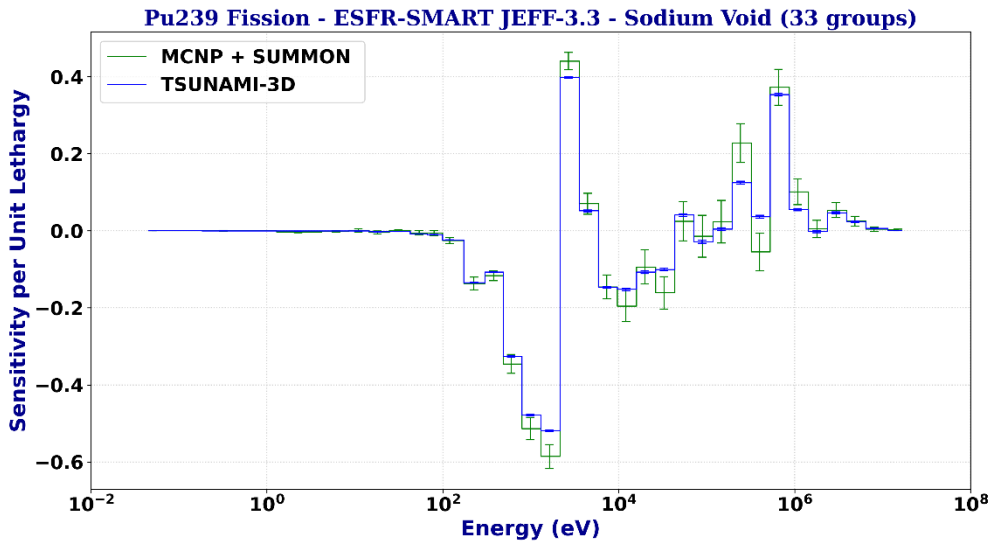


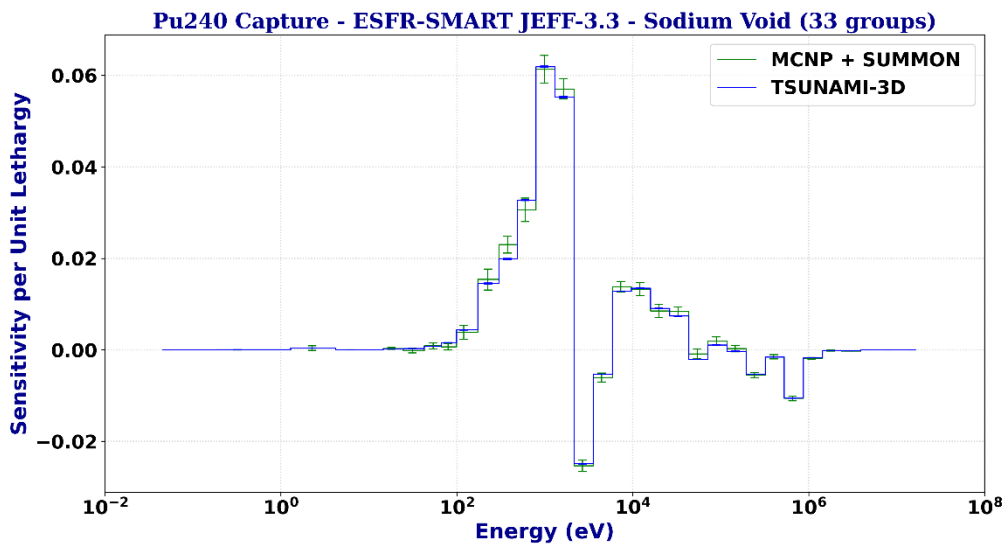
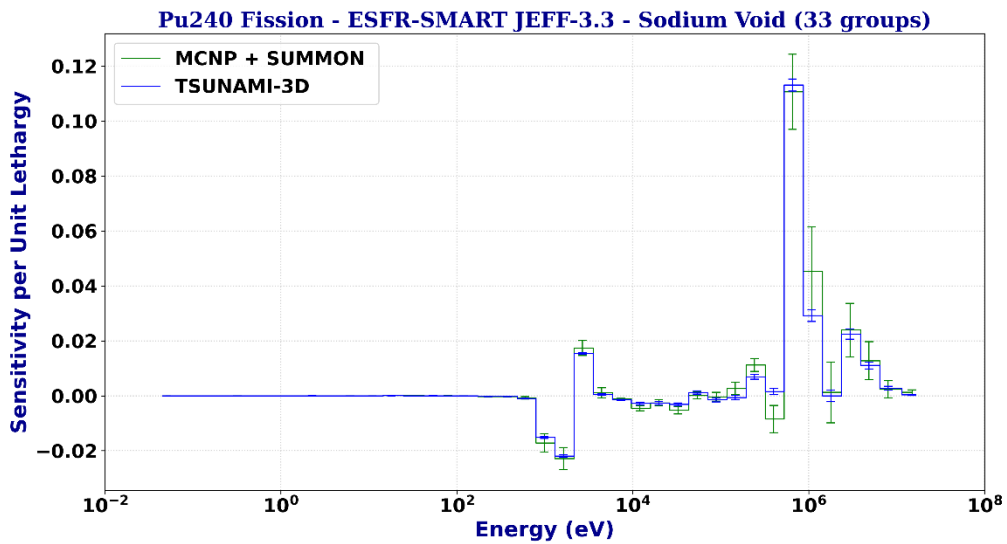
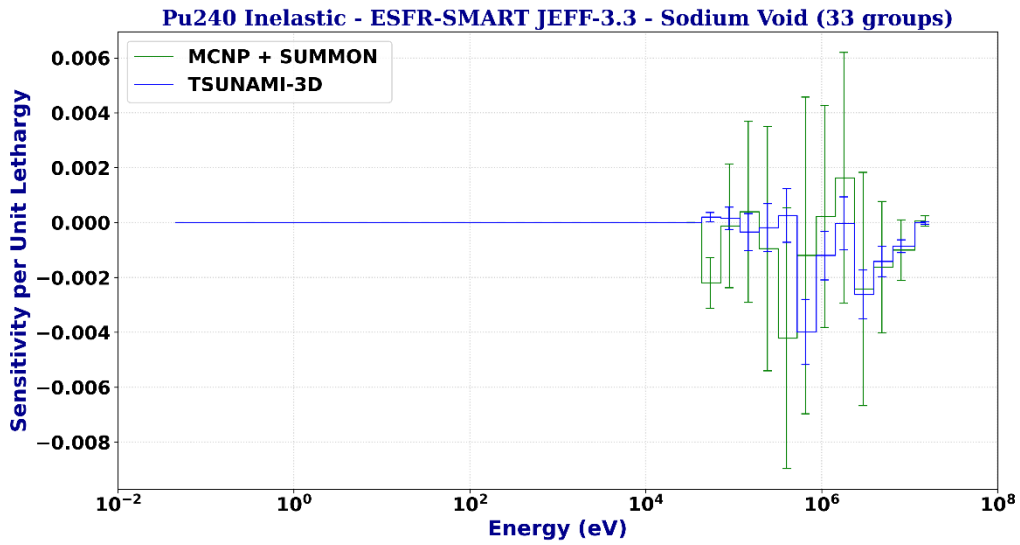




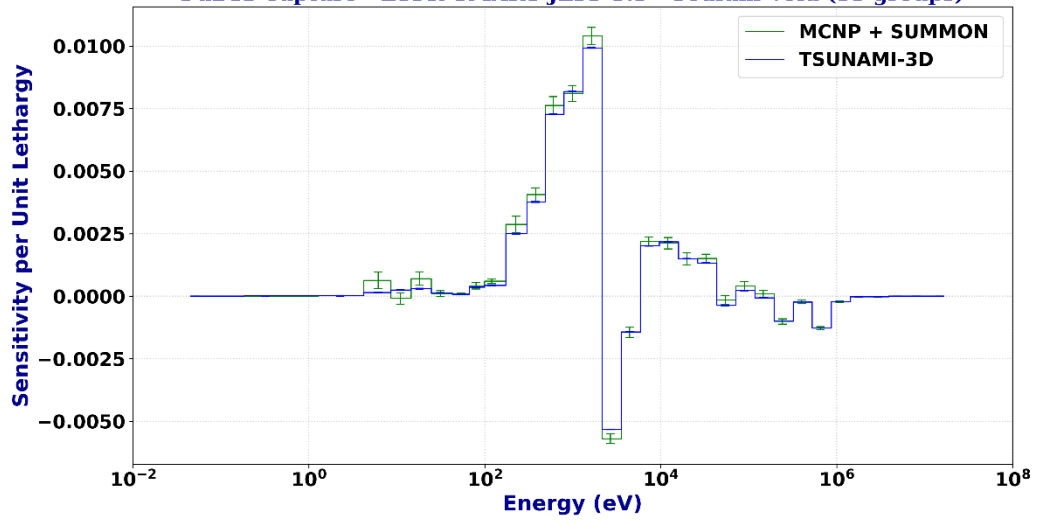








Pu241 Capture - ESFR-SMART JEFF-3.3 - Sodium Void (33 groups)



### Annex 3. Sensitivity data files supplied with this deliverable

The following files containing sensitivity profiles in the SDF format are supplied alongside with this report. They are available at [http://www.sanda-nd.eu/D5.1\\_sensitivity\\_profile\\_data\\_files](http://www.sanda-nd.eu/D5.1_sensitivity_profile_data_files).

- ESFR-SMART-EOC-RZ-JEFF33-KEFF-CIEMAT.sdf: sensitivity profiles (900K, 1200K and region-integrated) for the multiplication factor in 33 energy groups computed with MCNP6.2/KSEN using continuous energy JEFF-3.3 library.
- ESFR-SMART-EOC-RZ-JEFF33-SODIUM-VOID-CIEMAT.sdf: sensitivity profiles (900K, 1200K and region-integrated) for the sodium void in 33 energy groups computed with MCNP6.2/KSEN and SUMMON 2.4c using continuous energy JEFF-3.3 library.
- ESFR-SMART-EOC-RZ-JEFF33-KEFF-UPM.sdf: sensitivity profiles (region-integrated) for the multiplication factor in 33 energy groups computed with TSUNAMI-3D CE/SCALE6.2.3 using continuous energy JEFF-3.3 library.
- ESFR-SMART-EOC-RZ-JEFF33-SODIUM-VOID-UPM.sdf: sensitivity profiles (region-integrated) for the sodium void in 33 energy groups computed with TSUNAMI-3D CE/SCALE6.2.3 using continuous energy JEFF-3.3 library.
- ESFR-SMART-EOC-RZ-JEFF33-KEFF-IRSN-33g.sdf: sensitivity profiles (region-integrated) for the multiplication factor in 33 energy groups computed with MORET using continuous energy JEFF-3.3 library.
- ESFR-SMART-EOC-RZ-JEFF33-KEFF-IRSN-973g.sdf: sensitivity profiles (region-integrated) for the multiplication factor in 973 energy groups computed with MORET using continuous energy JEFF-3.3 library.

Be aware that the sensitivity profiles for some reactions, scattering reactions in particular (both elastic and inelastic) may have poor precision. Hence, they should be used with care.